



**Management Of Networked IoT Wearables – Very Large Scale
Demonstration of Cultural Societal Applications**
(Grant Agreement No 732350)

**D4.2 Validation of the ASFC and Noise Monitoring System
Configuration and Model Updating 2**

Date: 2018-12-28

Version 1.0

Published by the MONICA Consortium

Dissemination Level: Public



Co-funded by the European Union's Horizon 2020 Framework Programme for Research and Innovation
under Grant Agreement No 732350

Document control page

Document file: D4.2 Validation of the ASFC and Noise Monitoring System Configuration 2
Document version: 1.0
Document owner: DTU

Work package: WP4 – Acoustic Closed Loop Systems
Task: T4.1 – Loudspeaker Array Configuration
 T4.4 – Noise Annoyance Monitoring

Deliverable type: R

Document status: Approved by the document owner for internal review
 Approved for submission to the EC

Document history:

| Version | Author(s) | Date | Summary of changes made |
|---------|--|------------|--|
| 0.1 | Minho Song | 2018-12-10 | Initial manuscript |
| 0.2 | Daniel Plewe, Diego Caviedes Nozal, Minho Song | 2018-12-14 | Section 4, 5 are revised with recent experimental results. Figures and references are added. |
| 0.3 | Franz Heuchel, Minho Song | 2018-12-17 | Section 3.5 added with recent results. Section 3.2 and 5.1 revised. |
| 0.4 | Minho Song | 2018-12-18 | Revised section 2, 3, 4, and 5. |
| 0.5 | Minho Song, Franz Heuchel | 2018-12-20 | Revised section 3.6. Edited executive summary part regarding ASFC implementation. |
| 0.6 | Jonas Brunskog, Minho Song | 2018-12-20 | Index updated, Section 1 revised |
| 0.7 | Patricio Munoz, Minho Song | 2018-12-21 | Noise Annoyance part added. General revising. |
| 0.8 | Daniel Plewe, Diego Caviedes Nozal, Minho Song, Jonas Brunskog | 2018-12-21 | Executive Summary, Conclusion revised |
| 1.0 | Jonas Brunskog | 2018-12-28 | Final version, including corrections from review |

Internal review history:

| Reviewed by | Date | Summary of comments |
|------------------|------------|---------------------------------------|
| Claus Blaabjerg | 2018-12-21 | Reviewed ver0.6, with minor comments. |
| Peeter Kool CNet | 2018-12-27 | Accepted with minor comments |

Index:

| | | |
|----------|---|-----------|
| 1 | Executive Summary | 5 |
| 2 | Introduction | 7 |
| 2.1 | Purpose, Context and Scope of this Deliverable | 7 |
| 2.2 | Background..... | 7 |
| 2.3 | Tasks | 7 |
| 2.3.1 | Loudspeaker Array Configuration (Task 4.1)..... | 7 |
| 2.3.2 | Audience area loudspeaker array configuration – far field control (Task 4.1.1) | 8 |
| 2.3.3 | Quiet zones – near field control (Task 4.1.2)..... | 8 |
| 2.3.4 | Sound zone signal processing and optimization (Task 4.1.3) | 8 |
| 2.3.5 | Microphone Sensor Configuration (Task 4.2)..... | 8 |
| 2.3.6 | Sound Propagation Model and Parameter Updating (Task 4.3) | 8 |
| 2.3.7 | Noise Annoyance Monitoring (Task 4.4)..... | 9 |
| 3 | Audience area loudspeaker array configuration – far field control (T4.1.1) | 10 |
| 3.1 | Technology overview | 10 |
| 3.2 | Services enabled | 11 |
| 3.3 | Infrastructure and integration with the MONICA IoT platform | 11 |
| 3.3.1 | Information flow between ASFCS and MONICA IoT platform | 11 |
| 3.3.2 | Infrastructure and deployment of the ASFCS | 12 |
| 3.4 | Simulations | 14 |
| 3.4.1 | Assumptions | 14 |
| 3.4.2 | Setup..... | 14 |
| 3.4.3 | Summary..... | 19 |
| 3.5 | Measurements | 19 |
| 3.5.1 | Estimation of complex directivity point source model | 19 |
| 3.5.2 | Small scale anechoic experiment | 20 |
| 3.5.3 | Large scale outdoor experiment | 24 |
| 3.5.4 | Pilot Test: Kappa Futur Festival 2018 (KFF2018) | 26 |
| 3.5.5 | Pilot Test: Fredagsrock (Tivoli2018) | 29 |
| 3.6 | Future work..... | 30 |
| 4 | Quiet Zones – near field control (T4.1.2) | 31 |
| 4.1 | Technology overview | 31 |
| 4.2 | Services enabled | 33 |
| 4.3 | Infrastructure and integration with the MONICA IoT platform | 33 |
| 4.3.1 | Audio Signals from the Venue | 33 |
| 4.3.2 | Operational Status | 33 |
| 4.4 | Simulation | 34 |
| 4.5 | Measurements | 34 |
| 4.6 | Pilot Test at Tivoli | 36 |
| 4.7 | Future Work | 37 |
| 5 | Sound zone signal processing and optimization (T4.1.3 and T4.3) | 38 |
| 5.1 | Technology Overview | 38 |
| 5.1.1 | Sound Zone Signal Processing | 38 |
| 5.1.2 | Sound Propagation Model | 39 |
| 5.2 | Services enabled | 41 |
| 5.3 | Infrastructure and integration with the MONICA IoT platform | 41 |
| 5.4 | Simulations | 41 |
| 5.5 | Measurements | 42 |
| 5.5.1 | Weather and Sound Propagation | 44 |
| 5.6 | Future work..... | 49 |
| 5.6.1 | Sound Heat Map | 49 |
| 6 | Noise Monitoring System Configuration (T4.2 and T4.4) | 51 |
| 6.1 | Technology overview | 51 |
| 6.1.1 | Noise Monitoring System | 51 |
| 6.1.2 | Noise Annoyance Monitoring..... | 51 |

| | |
|---|-----------|
| 6.2 Services enabled | 52 |
| 6.3 Infrastructure and integration with the MONICA IoT platform | 52 |
| 6.4 Measurements | 53 |
| 6.5 Future work | 54 |
| 7 Conclusions..... | 55 |
| 8 List of Figures and Tables..... | 56 |
| 8.1 Figures | 56 |
| 8.2 Tables | 57 |
| 9 References | 58 |

1 Executive Summary

This report documents the first steps of the development of the Adaptive Sound Field Control System (ASFCS), the local Quiet Zone System (QZS), the Model Updating and the Noise Monitoring for the MONICA-project, all with the purpose to mitigate noise annoyance with neighbors and non-participating visitors during outdoor musical events, as well as to enhance the sound quality and musical experience of the audience. The report present simulations and measurements (pre-tests and pilot tests) in order to validate the chosen strategies. The report is an updated version of report D4.1, now covering also the findings and lessons learned form year 2 of the project, including pilot tests in Torino Kappa Futur Festival and Copenhagen Tivoli. Moreover, signal chains and protocols, as well as necessary hardware have been identified and documented.

The two important prerequisites of ASFC to perform well in the practical situation are 1) obtaining the accurate sound propagation model of the venue and 2) providing the suitable controlling signal through the secondary sources. The former is enabled using various sensors and microphones and the latter is done by monitoring the whole PA system output. Monitoring of electro-acoustic channels is a straight-forward task, but it is a difficult problem in practice. The signal format (analog or digital) and protocol (AES/EBU, MADI) change as passing equalizer or amplifier, and resulting different EQ/Delay filters are applied to each step. For this reason, sensible integration of ASFCS to the venue's PA system is needed. This year (2018), we introduced DANTE (Digital Audio Network Through Ethernet) protocol to ASFCS to avoid conversion between various signal formats and to manage long-distance transmission with a simple and reliable connection using standard network infrastructure. Also, to monitor different EQ/Delay filters and compression effect, we developed a high-power analog signal monitoring device called "Sniffer" which can monitor the end-signal from the PA amplifier.

The sound zone signal processing and optimization algorithm in ASFCS is based on the combined solution of Pressure Matching and Acoustic Contrast Control (PM-ACC). The PM-ACC solution fits well for the objective of the project because the sound field control in the dark zone must not negatively affect the sound experience in the audience area. From the large-scale outdoor pre-test in this year, we found out that even when the controlling secondary array (a set of loudspeakers) is located proximate to the audience (within 10m), an audience cannot perceive the negative effect from the sound source. Therefore, we could select the PM-ACC solution focus more on making the "contrast" effect.

Aiming for a very large scale cultural event, there should be some careful adaptation of the technique. Control of low-frequency band would require a regularization technique that gives a robust solution that can work in the outdoor conditions. Furthermore, 'large-scale' condition will impose various physically constraint real-time issues, leading modification of the given optimization scheme.

It is shown through simulations that the ASFS can considerably increase the difference in sound pressure level between the audience area and the venues surroundings in ideal environments. However, a compromise has to be made between the size of the control region in the neighbourhood and the equipment and computational modelling effort needed to cover a larger area. Comparing an extension mode of the ASFCS (only secondary sources being controlled, leaving the main PA uncontrolled) with a full mode (controlling both secondary and main PA sources) we can conclude that for a small dark zone, the benefit of using the full mode is small, but for the large dark zone, this benefit is essential, with an increase of the contrast of 10-15 dB. Moreover, it has been shown that due to model uncertainty, using model updating/machine learning techniques updating the propagation model will be essential for having a good result; a benefit of about 10 dB was found in the low frequencies.

Local quiet zones in loud environments can support communication and minimize the noise exposure of staff. Phone calls in emergency situations e.g. are an example of how even issues of safety can be supported. The challenge is to provide a zone of quiet close to a loud event area. While sound energy needs to be inserted in order to cancel the unwanted noise, such a system has to take that the surrounding area is not affected by disturbance introduced by the quiet zone controller. The system is made of active electronics which cancel out the low frequencies and a wall which blocks the high frequencies. In order to achieve the highest possible attenuation in the zone without interfering the surrounding optimized sound-field, the system has to be local. In that way the sound energy transmitted from the cancelling loudspeakers is kept within a dedicated region (as much as possible) and the passive barrier (the wall) can be smaller which reduces the size of the acoustic shadows.

Initial measurements of the Source Separation/Contribution techniques of the Noise Monitoring System have been successfully preformed.

In all, the initial validations of Adaptive Sound Field Control system as well as the Noise Monitoring configuration, using simulations and measurements, have shown positive results, but also indicating potential weaknesses to be aware of in the coming development.

2 Introduction

This chapter outlines the purpose, background and context of this deliverable as well as the structure of the remaining document.

2.1 Purpose, Context and Scope of this Deliverable

The objective of WP4 is to deploy components that can mitigate noise annoyance with neighbors and non-participating visitors during outdoor musical events. The main approach to do so is using an Adaptive Sound Field Control (ASFC or ASFCS)¹, consisting of loudspeaker arrays with an adaptive model updating system that adjusts for changes in climate and audience configuration. The ASFCS will be developed as a Sound Zone System (SZS) and will be integrated with the organizers Public Address (PA) system into the Acoustic Closed Loop System. The WP also contains a noise monitoring system. Data for the model updating of the ASFCS will be provided by stationary and wearable IoT sensors and apps. As such, WP4 is structured as follows:

- Task 4.1 Loudspeaker Array Configuration
- Task 4.2 Microphone Sensor Configuration
- Task 4.3 Sound Propagation Model Updating
- Task 4.4 Noise Annoyance Monitoring

This deliverable documents 'Validation of the Adaptive Sound Field Control (ASFC) for far and near field control, etc. (T4.1) and Noise Monitoring System Configuration'. The 'Noise Monitoring System Configuration' is located in Task 4.2 and 4.4; much of this task is however rather described in D4.4 'Precision IoT enabled Microphone Sensor 1'. The 'Sound Propagation Model Updating' of T4.3 is discussed in section 5 and the experimental results regarding temperature and wind speed is introduced. The documentation of the task 4.1 will be based on its three subtasks:

- Subtask 4.1.1 Audience area loudspeaker array configuration – far field control
- Subtask 4.1.2 Quiet Zone – near field control
- Subtask 4.1.3 Sound zone signal processing and optimization

2.2 Background

The WP will work on three physical scales: a) the external region – minimizing Annoyance; b) the audience area – maximizing Sound Quality²; and c) quiet zones within or close to the audience area – minimizing Loudness.

Most modern sound reinforcement systems are based on the line array principle, which allows for the control of directivity of the sound radiation of high and mid frequencies. However, the radiation of low frequencies cannot be as easily controlled, as sound waves at these frequencies are less attenuated by air and reflections from boundaries and are damped the least by the structures of residential buildings. Low frequencies are therefore the most critical frequencies in the noise problem of outdoor concerts. As controlling the sound field over large areas with a feasible number of loudspeakers is restricted to low frequencies, tackling the low frequency problem with this method is appropriate.

2.3 Tasks

The tasks in WP4 is here described shortly (mostly corresponding to the text in ANNEX 1 (part A)).

2.3.1 Loudspeaker Array Configuration (Task 4.1)

As current PA systems are designed primarily with the coverage in the audience area in mind, improvements can be achieved not only by adding control sources, but also by reconfiguring the main PA design in light of

¹ The abbreviation ASFC is used denote the concept of the method. For the physically implemented system, ASFCS is used.

² Sound Quality here includes several perceptual dimensions, including Loudness, Directivity, Distortion, Echoes etc. In this project, good sound quality in audience area means not disturbing the sound made by sound engineers for the concert.

the new performance requirement, as it will influence on the number of control sources needed and the achievable attenuation. Therefore, the MONICA ASFCS, consisting of the main PA and additional control sources, will be optimized as a complete system. At high frequencies (HF) the sound field control might be combined with passive solutions (absorbers and screens) – at least the quiet zones.

2.3.2 Audience area loudspeaker array configuration – far field control (Task 4.1.1)

This subtask addresses the ASFC of the external region as well as the audience area. In addition to the existing PA system loudspeakers, loudspeakers will be added to control the sound level in the external zone. The PA system input signals will be fed into the ASFCS for further use. At low and mid frequencies (LF/MF), an ASFCS will be deployed, using the concept of sound zones. The ratio of the acoustic energy in ensonified³ zones to the acoustic energy in a quiet zone will be maximized, with maintained sound quality in the ensonified audience area. Also, the loudspeaker configuration and location will be optimized. The current meteorological conditions need to be taken into account in the control loop, described in T4.3.

2.3.3 Quiet zones – near field control (Task 4.1.2)

Within or very close to the audience area, smaller quiet spots will be created, intended for security personnel and for conversation spots. It is here crucial to not generate acoustic interference outside the quiet spot area, in order to preserve sound quality in the audience area. Therefore, the near field of smaller acoustic sources will be used: a) only a moderate acoustic power is needed to obtain an effective reduction, b) the interference effects far from the control region are minimized, and c) it will result in spatial stationarity, i.e. a quiet zone that is not moving depending on changing atmospheric conditions.

2.3.4 Sound zone signal processing and optimization (Task 4.1.3)

The ASFC task is an optimization problem. The overall cost function will be combinations of minimizing annoyance at external regions, maximizing sound quality (e.g., perceived directionality and intended loudness) in the audience area, and minimizing loudness in the surrounding areas. Good estimates of the transfer functions between source and receiver positions are essential, as developed in T4.3. The signal processing is a combination of Acoustic Contrast Control combined with Pressure Matching (*PM-ACC*). In order to go from present state technology in rooms to real outdoor event conditions, the underlying optimization problems should be developed to minimize the radiation to the surrounding. To have 'escape' for the produced sound power and to have more degrees of freedom for the optimization, radiation upwards is allowed, but not to the side (3D zones). The concept of robust optimization will be useful, taking into account uncertainties in sensor input and forward modelling.

2.3.5 Microphone Sensor Configuration (Task 4.2)

High quality and accurate microphones, which can withstand the weather, will be developed into IoT enabled microphone devices. To be consistent with the concept of IoT and to be able to exploit this device for other applications, it will be developed as a generic sound level meter connected to the Internet, discoverable online by applications, and being able to provide information on deliverable data and location. It is annotated with semantic information so that applications can select them on or off, both during the programming of applications and during run-time. In this way, administrators can set up different sound meters ad hoc and applications can find the exact location of these devices. As an example, it can be used for identifying and monitoring noise sources in public, as in T4.4. The IoT enabled microphone is mainly described in Deliverable D4.4 and D4.5.

2.3.6 Sound Propagation Model and Parameter Updating (Task 4.3)

The forward model in T4.1.3 needs to be updated to match the actual atmospheric/weather conditions, by use of adaptive filters and Bayesian statistical methods. The forward model is based on *Nord2000* (Plovsing, 2006), used for predicting outdoor noise propagation. It includes major mechanisms of attenuation for any terrain shapes including screens. It will be usable as is when estimating the Sound Pressure Level (SPL) at the affected neighbour's position, but for the transfer function estimate in the audience area it has to be adjusted. Information of the current situation will be provided using the inputs from the distributed IoT sensors, including

³ With 'ensonified' is meant an area with an enhanced sound field, filled with sound. Compare with illuminated for light.

distributed climate sensors (temperature, wind, humidity). For the audience area, the audience absorption and scattering is of high importance. To estimate these data, a mapping of the density of the spectators, and notification of significant changes in this, will be done using video cameras and image processing. A mapping of SPLs obtained from a dense network of high quality calibrated sensors supplemented with additional data from cheaper uncalibrated sensors from available wearables. Subjective feedback information from users regarding sound quality and annoyance, via mobile phone apps, will also be included in the dataset – mainly used for the decision support system, T6.3.

2.3.7 Noise Annoyance Monitoring (Task 4.4)

To monitor the neighbours' annoyance and the audience acoustic comfort, it is necessary to separate the different source contributions in the signal at a given location. Two general strategies will be used, depending on the distances between sensors and information available. For IoT devices correlation-based approaches can be used via access to the source signal, and depending on the location of the sensor combined with the propagation model in T4.3. In other cases, when only isolated microphones are available, machine learning techniques will be used. Noise annoyance metrics will be calculated for each separated source based on the outcome of the source separation techniques. The measured input data comes partly from IoT devices distributed at the neighbours' position, and partly from the sensors developed in T4.2. Feedback information from users regarding sound quality and annoyance, via mobile phone apps T6.5, will also be included in the dataset. The subjective data obtained by the survey will be analysed by experts in T10.2.

3 Audience area loudspeaker array configuration – far field control (T4.1.1)

3.1 Technology overview

Traditional loudspeaker systems for outdoor sound reinforcement typically consist of two loudspeaker line arrays and a set of subwoofers arranged in a horizontal array or as two left-right clusters. In the ASFC, these systems (*primary sources*) are extended by the use of additional low-frequency loudspeakers (*secondary sources*). These are placed behind the audience in between the primary sources and the neighboring region in which the sound from the event should be reduced (*dark zone*). The method of creating spatially separate acoustical zones is often called sound zoning (see e.g. the review by Betlehem et al, 2015).

A sketch of the setup is shown in Figure 1. The basic idea is to optimize the radiation from the secondary sources in such a way, that the sum of sound pressures from the primary and secondary sources effectively reduces the total sound pressure level in the dark zone. Use of additional loudspeakers to control the sound in the dark zone must not negatively impact the sound experience in the audience area, the *bright zone*. This restriction must be included in the loudspeaker configuration design by either using directive loudspeakers facing away from the bright zone for the secondary sources or in the formulation of the loudspeaker signal optimization problem (see Chapter 5, Sound zone signal processing and optimization).

A well performing ASFCS will enable a high sound pressure level in the bright zone relative to the sound pressure level in the dark zone. A performance indicator for this problem is the *acoustic contrast*, which is the difference of the mean SPL in the bright zone to the mean SPL in the dark zone (Choi and Kim, 2002).

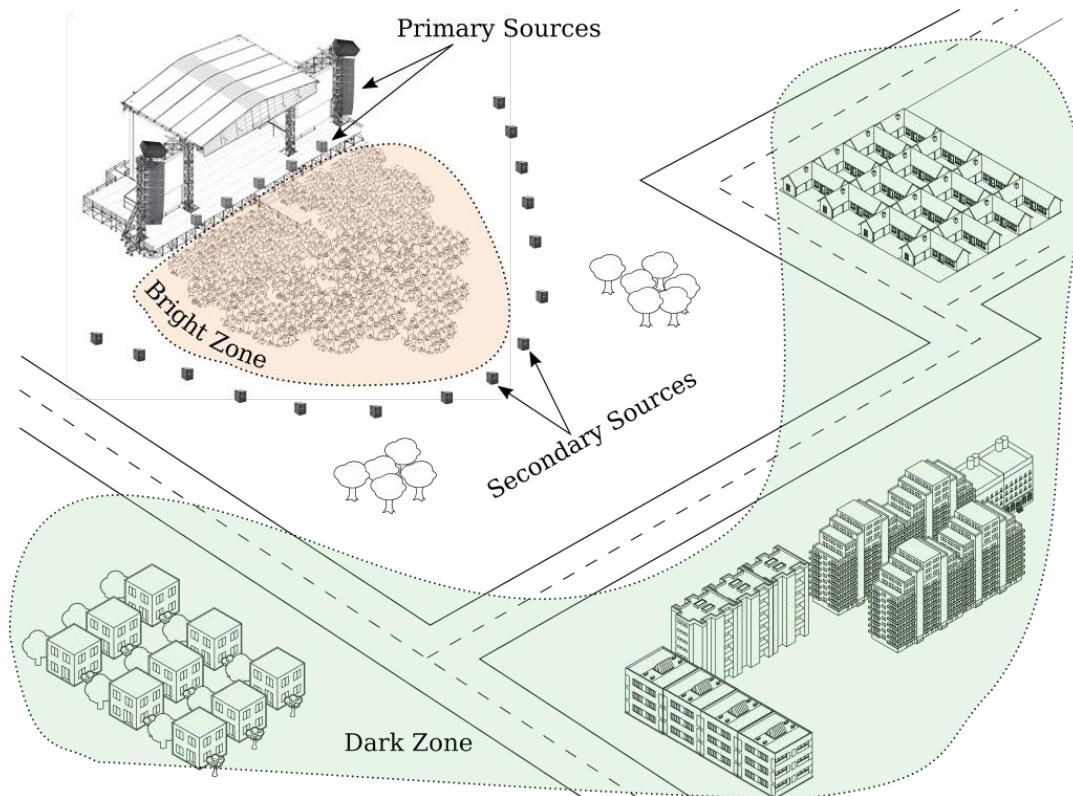


Figure 1: Sketch of the adaptive sound field control system, which is optimized for a good audio experience in the bright zone and low sound pressure level in the dark zone

The ASFCS can be implemented in two modes: in the *extension mode* described above, the ASFCS only controls the secondary sources. This mode of operation is a natural approach in the development of the ASFCS because 1) fewer sources are controlled, and 2) sound engineers will be less skeptical because the main system is left untouched except for the monitoring purpose. Moreover, 3) in case of failure, the system can be easily shut off without interfering with the main system.

In the second mode of operation, *full mode*, both the primary and secondary sources are optimized by the ASFCS. Using the additional degrees of freedom (more loudspeakers) will enable a larger acoustic contrast and optimization of the sound field within the audience area. However, this poses the non-trivial question of a perceptually ideal sound field in the audience area. In case of failure, the ASFCS can be bypassed and the sound reinforcement system used in its default mode. Table 1 compares the two operation modes.

| Extension Mode | Full Mode |
|---|--|
| Only secondary sources are controlled | Both primary and secondary sources are controlled |
| SPL in dark zone is minimized | SPL in dark zone is minimized and sound field in audience area optimized |
| More easily accepted by sound engineers | Acceptation questionable |
| Shut off in case of failure | Bypassed in case of failure |
| Information on full system needed | Information on full system needed |

Table 1: Comparison of operation modes

The ASFCS must be distinguished from generating *Quiet zones* (Task 4.1.2, see the section 4). The former technology controls sound in a large area and is based on sound zoning techniques, while the latter controls the sound in a very confined area and is based on adaptive filtering and active noise control.

3.2 Services enabled

The ASFC solution aims to provide an optimized sound field in the audience area and minimizes the impact on neighboring areas. The ASFCS consists of specific hardware which needs to be added to a venue's sound system. The software (sound field optimization algorithm and sound propagation model) is developed and tuned specifically for each venue. The ASFC solution is related to the following use case:

Sound Level Adjustment:

- The ASFC provides an optimized sound field in the audience area and minimizes the impact on neighboring areas

3.3 Infrastructure and integration with the MONICA IoT platform

3.3.1 Information flow between ASFCS and MONICA IoT platform

The ASFCS interacts with the MONICA IoT platform in two ways:

1. The MONICA platform provides various collected sensor data (e.g. weather condition and sound pressure) to the ASFCS upon requests, which is used to update the sound propagation model and estimate the sound propagation in and around the venue.
2. The sound propagation model supplies information on the sound condition - in and around the venue - to the MONICA IoT Cloud in form of a Sound Heat Map (the sound propagation model behind the Sound Heat Map is described in Chapter 5).

Figure 2 shows a schematic of the information flow in the acoustic closed loop system. Compared to a traditional sound reinforcement chain, we insert a *Sound Field Controller*, which is a processing unit in between

the mixer and the loudspeaker system, which computes the optimal loudspeaker signals. IoT enabled microphones and weather sensors distributed throughout the venue and the control areas continuously measure the sound pressure field created by the ASFCS and current weather conditions. This data is made available to the *Sound Propagation Module* via the MONICA IoT platform. The Sound Propagation Module uses this data to estimate the transfer-functions between sound sources and the control areas, which are needed by the Sound Field Controller's optimization routine.

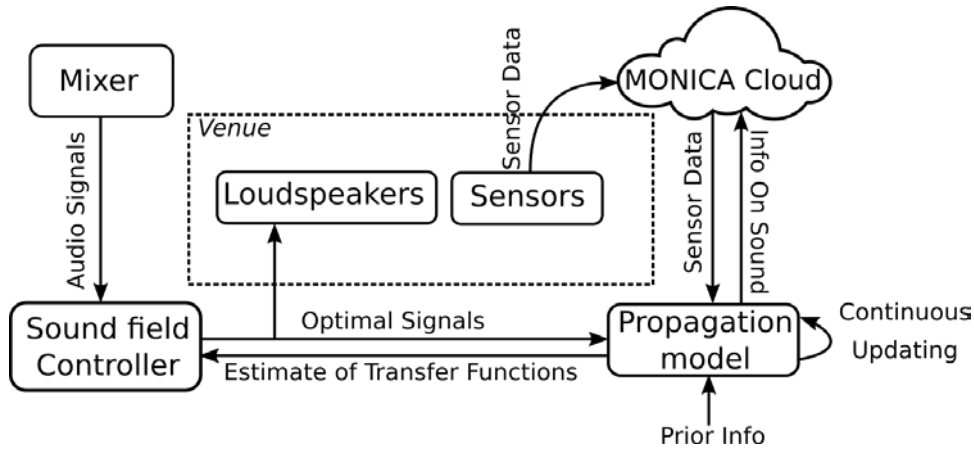


Figure 2: Information flow in the sound field control system

3.3.2 Infrastructure and deployment of the ASFCS

3.3.2.1 Extension mode versus Full Mode

In practice, the ASFCS will be deployed as shown in Figure 3. The Sound Field Controller and Propagation Model modules are running on a local processing unit called *ASFCS core* (high-performance computer with audio processors and interfaces), which also handles the communication to the MONICA cloud either over Ethernet or WIFI connection. Optionally, wired microphones can also be connected to the processing unit. In Full Mode, the mixing signals are directly fed to the processing unit and from there to the loudspeaker system. In Extension Mode, the signals from the mixing board are fed both the primary sound system and ASFCS processing unit. The ASFCS is set up, monitored and controlled directly through the processing unit.

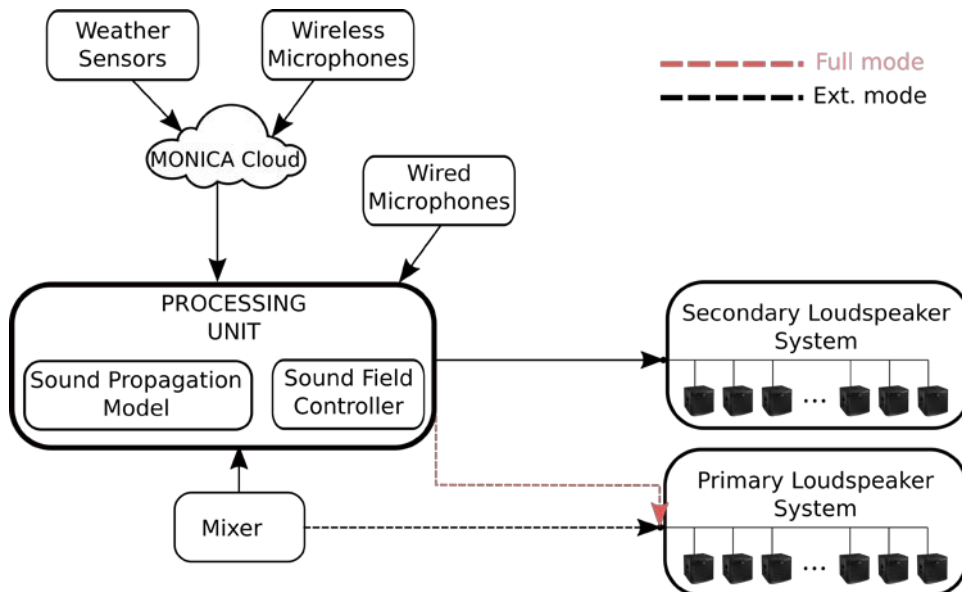


Figure 3: Infrastructure and deployment of the ASFCS. In full mode the primary loudspeaker system is fed from the Processing Unit. In the Extension Mode the primary loudspeaker system is fed directly from the mixer

3.3.2.2 Infrastructure and signal flow of the ASFCS

The infrastructure and signal flow of the ASFCS is described in Figure 4 (with pilot Tivoli as an example). *ASFCS Core* is a processor that generates Sound Heat Map and calculates optimized driving solution from MONICA cloud. When the core also performs as a signal renderer (signal filtering), it should be connected to the signal hub (*Audio Interface*) and receive the input signal. If separate DSP is used, then the Core is only used as a solution generator. The Audio Interface is the hub of the ASFCS, receives monitored signal from router or preamp (for closed-loop control) and finally delivers the signal to Core or DAC. Mic Preamp/ADC or Router are used as the gateway of ASFCS, receives a signal from the PA system or microphones. These gateways also deliver the control signal to the main PA system in the use of Full mode. Note that the *Secondary Loudspeaker System* needs to deliver comparable energy level with the main PA system.

The red dotted line in Figure 4 represents audio analog signal flow over DANTE (Digital Audio Network Through Ethernet) protocol and the dotted line is for the digital signal flow using AES/EBU or MADI protocols. The triple compound line denotes multiple parallel cables are required to connect between two nodes. On the other hand, the simple line represents a simple delivery of the multichannel signals through a single cable (e.g. MADI). We selected the DANTE protocol for connecting ASFCS components because the distances between ASFCS components can be very long compared to the standard audio device setup. To ensure the reliable signal transmission over several hundreds of meters, signal routing over Ethernet cable is the most suitable approach. ASFCS requires monitoring a high number of PA channels, but this can be easily done when the DANTE protocol is used. Once the signals are on the DANTE network using any DANTE-enabled device, now they are ready to be controlled.

In Figure 2, the Sound Field Controller requires monitoring the audio signal (Music playing in Figure 4) from the mixer in order to generate the optimal signal. It is important to note that the signal output from the Primary Loudspeaker System can be different from the PA Mixing Console output. Generally, after the music signal passes the mixing console, there are EQ/delay filters applied afterward which are selected to fit the specific venue. For accurate monitoring, it is recommended to monitor the whole electro-acoustic signal from the last node (Monitoring Path 2 in Figure 4). In this case, all analog channels from the PA amplifier should be fed to ADC in ASFCS. In 2018, we have developed a device called *Sniffer*⁴ which can monitor the analog output (The monitoring path 2) from the PA amplifier. Instead, the monitoring can be done at the previous nodes (Monitoring Path 1) if the transfer function to the end node is known in advance. In this case, digital monitoring outputs are fed into any DANTE-enabled devices in ASFCS. If there is no possibility of change in transfer function during the event, the latter approach can be practical but if not, the final node after the PA amplifier should be monitored. For the Full mode, the control signals to Primary Loudspeaker System is delivered from the Router of ASFCS through the inverse path of monitoring.

⁴ The Sniffer is a hardware device developed by DTU for the MONICA project. It is placed in the signal line between the PA amplifier and the PA loudspeaker, and thus monitor the signal actually provided to the loudspeaker. This signal is sent to the DANTE interface for further processing, see Figure 4.

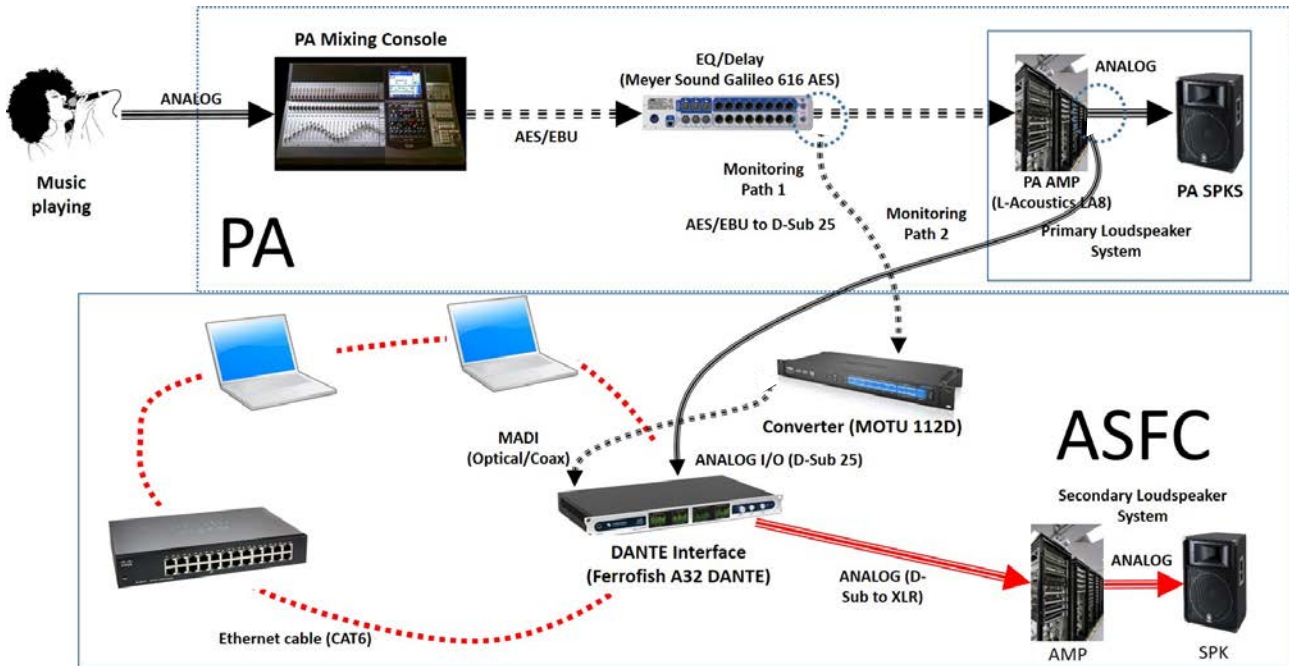


Figure 4: Example of ASFCs connected with PA system of the pilot at Tivoli

3.4 Simulations

The sound field control principle is validated here with two sets of simulations for a simple case resembling a small, open-air concert setup in which the radiation of sound to a sensitive area 1) around the concert or 2) behind the concert is to be mitigated. These two cases are useful in illustrating the differences between operation in extension mode and full mode. Similar results have been already published by the authors in (Heuchel and Caviedes, 2017).

3.4.1 Assumptions

The simulations that shown here make the following assumptions:

- The transfer-functions between control sources and control areas are known precisely. However, the sound propagation model will be responsible to compute accurate enough estimates of these transfer-functions in practice.
- The conditions do not change and thus, the transfer-functions are constant over time. In practice, changing conditions like weather or size of an audience will change over time and the sound propagation model has to adapt continuously to these changes.
- The loudspeakers can be modeled as omnidirectional monopole sources. Real loudspeakers have complex radiation patterns, which can be modeled in the future by using a complex directivity point source model (Feistel, 2014).
- The geometry of the venue consists only of plane grounds. Real venues have a high geometrical complexity which will be modeled in the future by the sound propagation model.

3.4.2 Setup

The simulation setup is shown in Figure 5. The *surrounding dark zone* resembles the problem of Figure 1 and the *small dark zone* illustrates a case where there is only a specific, local area with a noise issue. The primary sources resembling the conventional sound reinforcement system are modeled by a horizontal array with 6 loudspeakers. The 12 secondary sources are placed below the bright zone in form of two lines with 6

loudspeakers each. The double layer array can act as a combination of monopole and dipole sources that mainly direct their sound energy away from the bright zone.

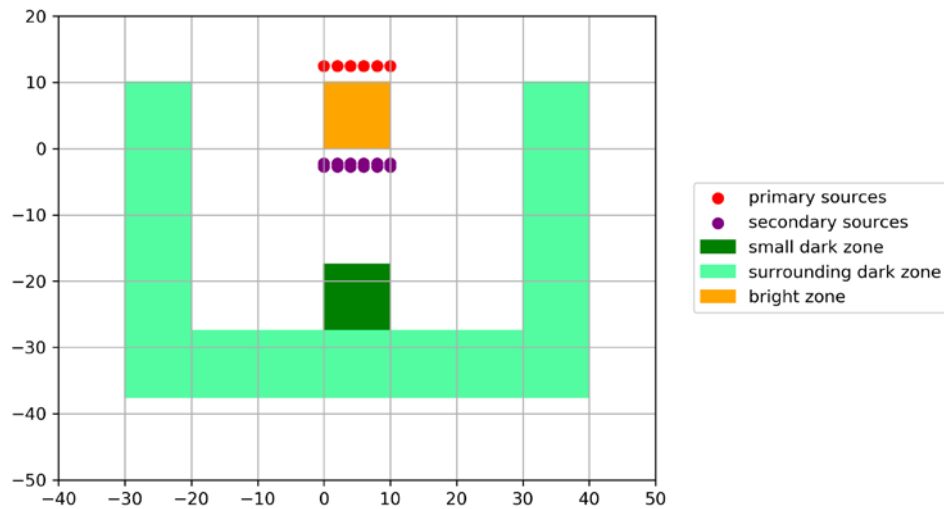
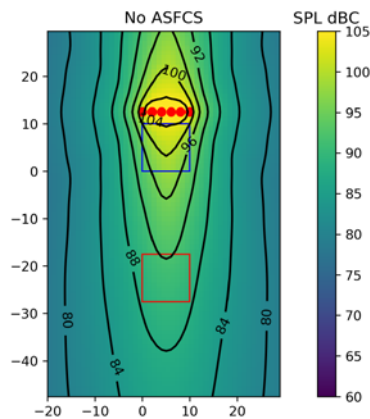


Figure 5: Sketch of the adaptive sound field control system, which is optimized for a good audio experience in the bright zone and low sound pressure level in the dark zone

The frequencies of interest are the bass frequencies ranging from 20 to 250 Hz – in the simulations below the frequency range is however limited to 20 to 150 Hz. The sources are placed at a height of 0.4m while the bright and dark zones are sampled at a height of 1.6m. The ground is considered a compacted park area (Impedance Class E according to Nordtest) with flow resistance $\sigma = 700 \text{ kPa} \cdot \text{m/s}$. The speed of sound is $c = 343 \text{ m/s}$ and air density $\rho = 1.2 \text{ kg/m}^3$. The loudspeakers are modeled as monopoles with constant magnitude response. To optimize the loudspeaker driving signals, one needs to know how the driving signals are related to the sound pressure in the control zones. This relationship is described by the *transfer-function*. In this simulation this transfer-function is obtained by sampling the control zones at 2.5 points per maximum wavelength in each direction and computation of the transfer-function between sources and the sample positions using the *Nord2000* propagation model (Plovsing, 2006), see further in section 5.1.2.



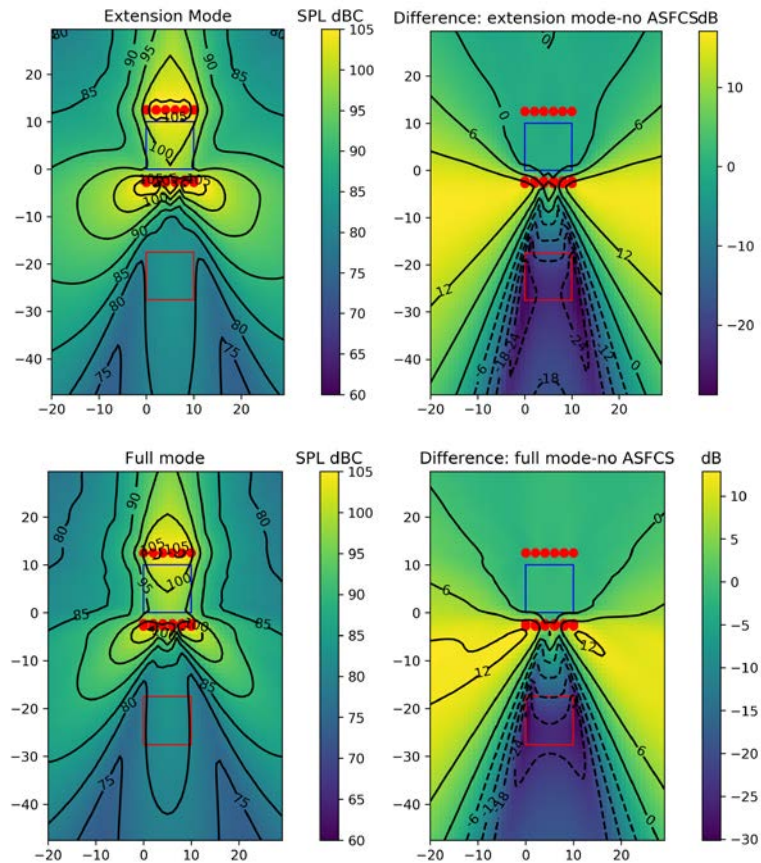


Figure 6: Comparison of total sound pressure level in the vicinity of the simulated venue, small dark zone.⁵

3.4.2.1 Small dark zone

Figure 6 shows plots of the total SPL around the simulated venue for the three cases

1. Without ASFCs: the primary sources are playing with constant gain. This is the equivalent to a conventional sound reinforcement system
2. Extension Mode: only the secondary sources are controlled by the ASFCs, while the primary sources are driven as in case 1
3. Full Mode: all sources are controlled by the ASFCs. The target field in the audience area is the sound field of case 1

Together with SPL comparison between case 1 and cases 2 and 3. Both full and extension mode create a similar SPL map with an area of destructive interference close to the dark zone, while at the same time increasing the SPL in other areas, which are not controlled. This is a classic result of sound power interaction of coherent sources. In free-field, a control source has to be closer than half a wavelength to a noise source to be able to reduce the total emitted sound power effectively, see e.g. (Jacobsen and Juhl, 2013). The secondary source array will thus not work as an active absorber, but rather create destructive interference in some area at the expense of higher sound pressure levels at other positions. Care must be taken in designing the loudspeaker arrays and optimization problem, such that the reduction of noise levels in the dark zone does not lead to new noise problems in other areas.

Figure 7 shows a comparison of the achieved acoustic contrast between bright and dark zones over frequency. The ASFC increases the acoustic contrast considerably over the whole frequency range. Extension and full modes give very similar results.

⁵ Note that dBC is used in Figure 6 and Figure 8 as it better corresponds to the perception of loudness for loud sound events. The dB difference figures are however independent of the frequency weighing. Also not that what is called 'Difference' here is called 'Insertion Loss' (IL) in other part of this document.

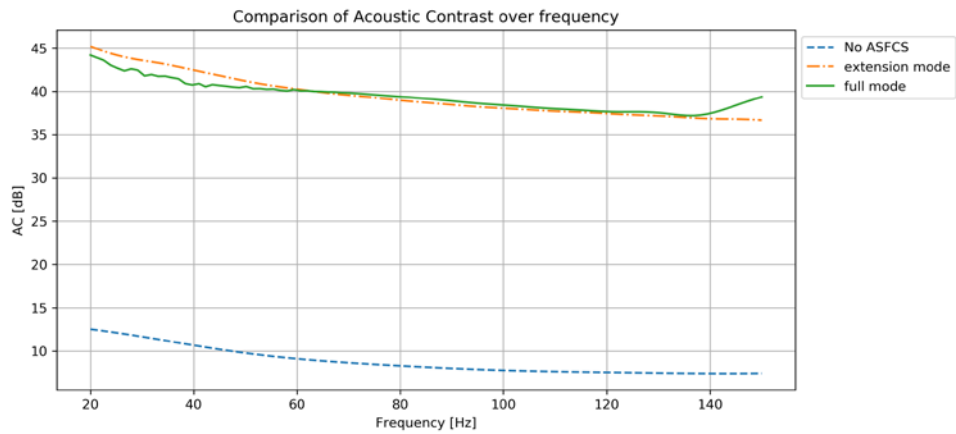
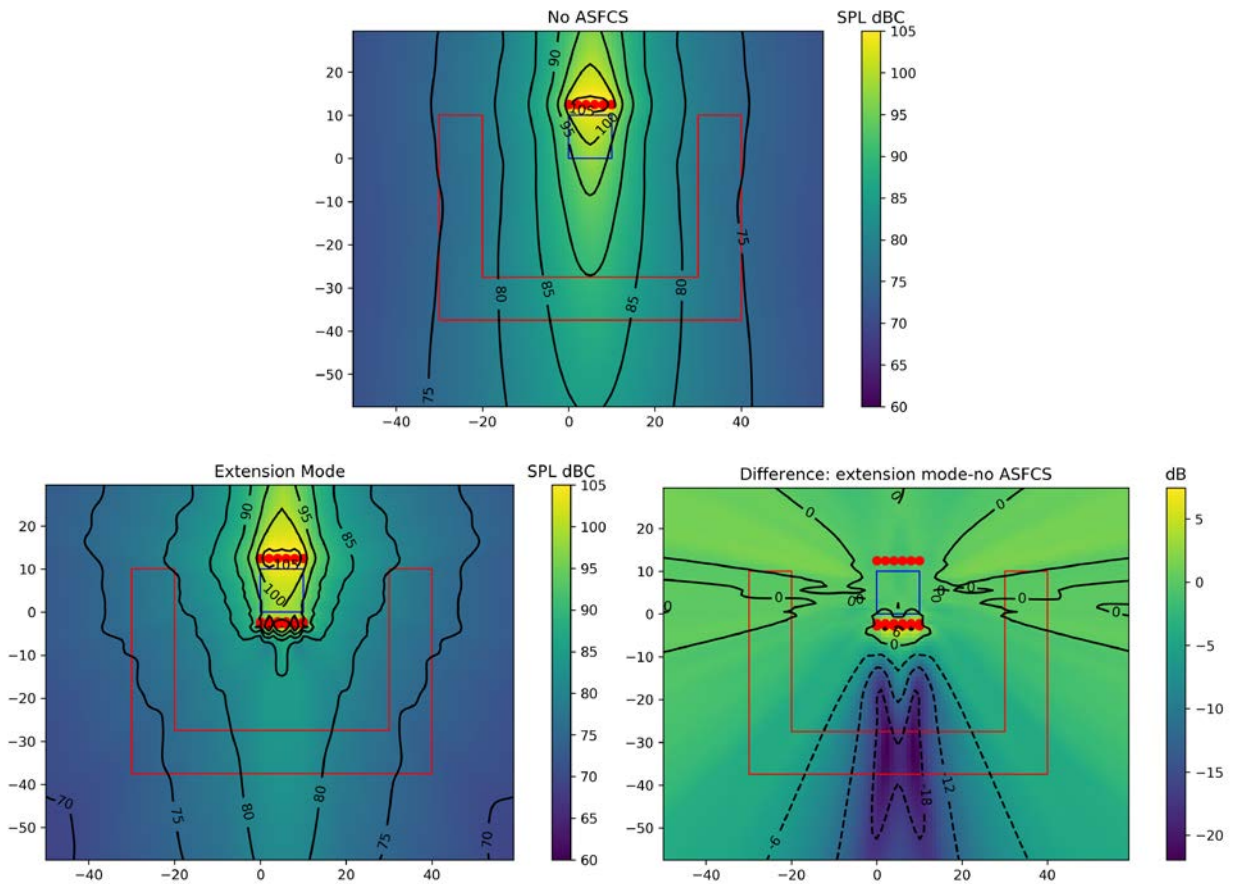


Figure 7: Comparison of total sound pressure level in the vicinity of the simulated venue for the small dark zone case

3.4.2.2 Surrounding dark zone

Figure 8 shows plots of the total SPL around the simulated venue for the three cases "No ASFCs", "Extension Mode", "Full Mode", analogous to Figure 5. In extension mode, the reduction of SPL is focused on the area below the secondary sources, while a full control enables the reduction in most of the vicinity due to a stronger directivity of the primary array on to the bright zone.



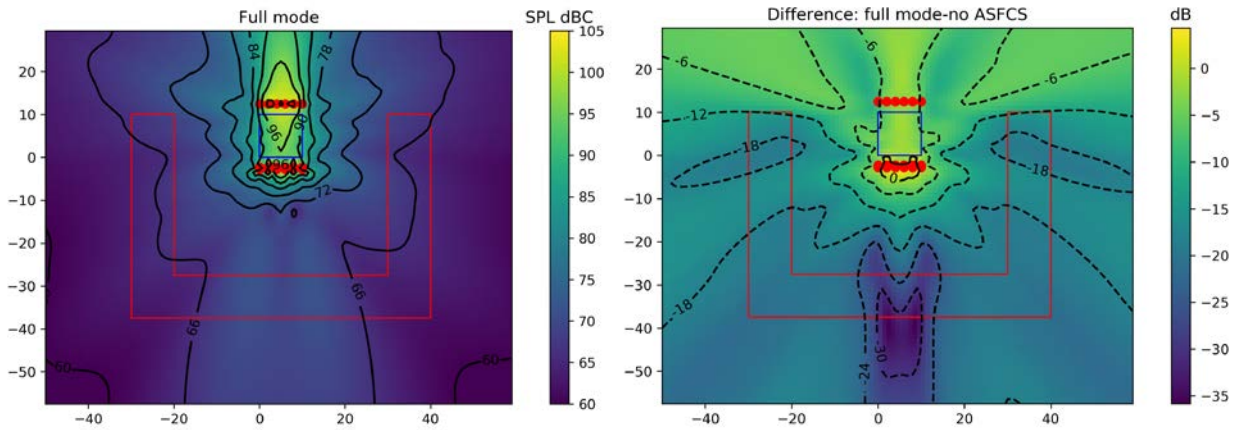


Figure 8: Comparison of total sound pressure level in the vicinity of the simulated venue, surrounding dark zone

Figure 9 shows a comparison of the achieved acoustic contrast between bright and dark zones over frequency. The ASFC in both full and extension mode increases the acoustic contrast over the whole frequency range, with the full mode leading to a larger mean contrast, because the SPL is reduced in a much larger area.

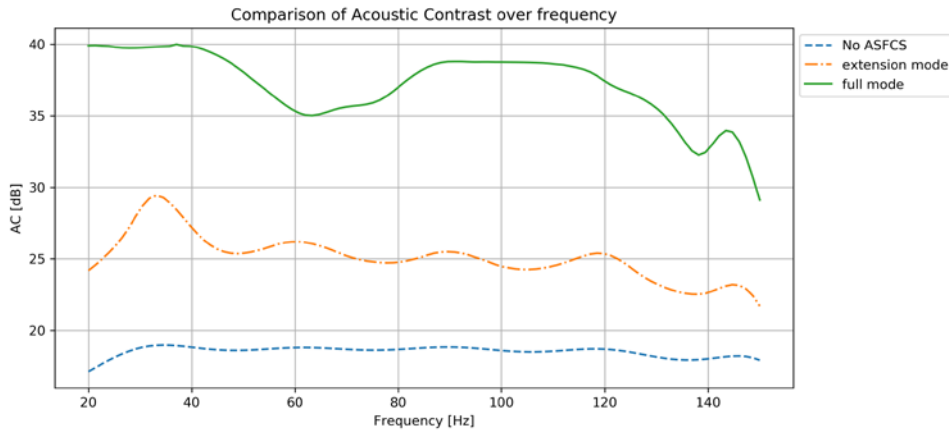


Figure 9: Comparison of total sound pressure level in the vicinity of the simulated venue for the surrounding dark zone case

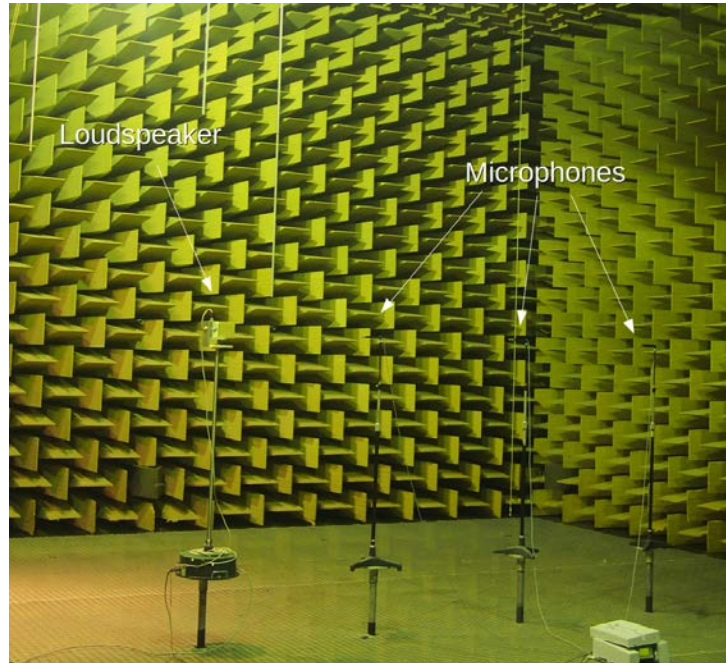


Figure 10: Measurement setup for loudspeaker characterization

3.4.3 Summary

The above simulations show that the ASFCs can considerably increase the acoustic contrast between audience area and venue's surroundings. Larger dark zones and control over more sources are helpful in reducing the SPL spill into neighboring regions. However, this comes at the cost of increased complexity. A larger dark zone needs more microphones to observe the sound field and more sources lead to a higher computational effort in the optimization problem. While a larger (e.g., surrounding) dark zone will always lead to a larger area of reduced SPL, control over more sources does not always lead to an increased contrast, as was seen in Figure 7. Moreover, Comparing Figure 7 and Figure 9, we can conclude that for a small dark zone, the benefit of using the full mode is small, but for the surrounding dark zone, this benefit is essential, with an increase of the contrast of 10-15 dB.

3.5 Measurements

In 2017, only preparation measurements for the characterization of loudspeakers was completed (see section 3.5.1). In 2018, the sound field control system was experimentally studied and tested in a variety of configurations. We present here results from one experiment under controlled conditions (section 3.5.2), one large-scale outdoor test (section 3.5.3), and two pilot tests (section 3.5.4 and 3.5.5). Results of these measurements have already been the basis for a conference publication (Heuchel et al., 2018). The second pilot test was not successful and we are describing the issues in section 3.5.5.

3.5.1 Estimation of complex directivity point source model

The sound propagation model uses Complex Directivity Point Sources (CDPS) as simplified models for the loudspeakers (Feistel, 2014). A measurement procedure has been developed, that finds the best fit of a loudspeaker to the CDPS model, such that it can be used in the sound propagation model.

A setup of the procedure, deployed in the large anechoic chamber at DTU, is shown in Figure 10. The loudspeaker under test is a small test loudspeaker with a 4-inch driver. It is mounted on a turntable, such that its frequency-response can be simultaneously measured over different radiation angles at three microphone positions using the swept-sine technique (Farina, 2007).

The loudspeaker's directivity dependent frequency-response is measured and fit to a CDPS model. A comparison between measured and modelled response is shown in Figure 11. One can see that the absolute

pressure and phase of the loudspeaker can be reproduced by the fitted CDPS model with a relative error of up to 25%, equivalent to 2 dB. While this shows that the source can be modelled as a CDPS at all frequencies and directions, there is still a considerable error considering that the test is done under ideal conditions.

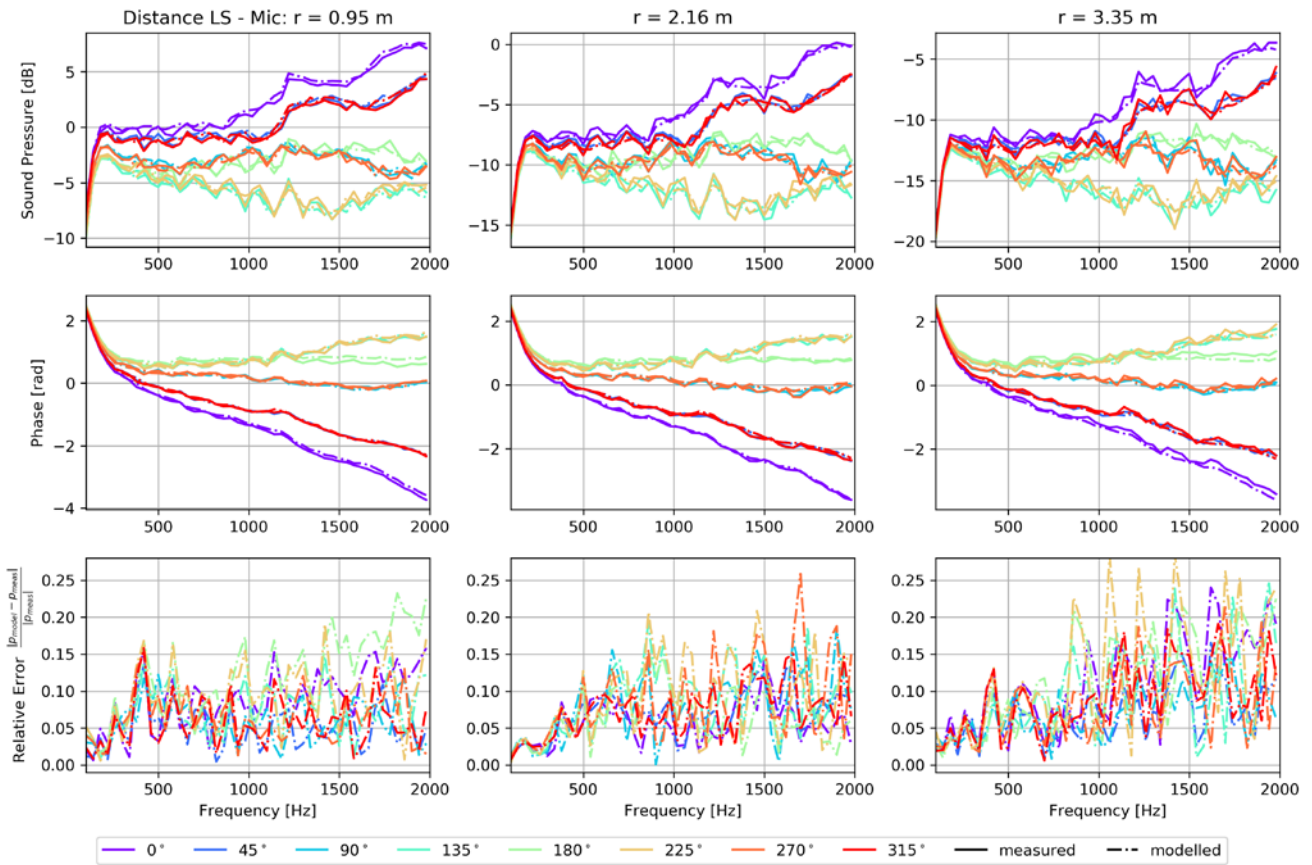


Figure 11: Modelled and measured response of the loudspeaker under test at the microphone positions together with the relative error. Note that the phase is back-propagated in time and unwrapped for a clearer presentation and readability.

3.5.2 Small scale anechoic experiment

The goal of this experiment was to test the sound zoning system and the implementation of transfer function measurement and filter computation routines in controlled conditions. This is a downscaled experiment (factor ~ 1:5 – 1:10) and we are looking thus at a higher frequency range. At a larger scale, the insights of this experiment will still be valid, but for a lower frequency range. The basic configuration of the loudspeaker array is very similar to what was later used in the full scale outdoor tests.

3.5.2.1 Experimental setup

Figure 12 shows the small-scale experimental setup in the anechoic chamber of the Technical University of Denmark. Six primary sources are simulating the subwoofer array of a typical sound reinforcement system. Behind the bright zone (the audience area), a secondary loudspeaker array consisting of 12 sources is placed in a double layer array with 6 loudspeakers facing the bright and 6 loudspeakers facing the dark zone. Directly behind the secondary sources, a dark zone is simulating a sensitive neighboring area.

We measured the transfer functions from all loudspeakers to a densely sampled grid of 700 microphone positions per zone to construct the transfer function matrices. The transfer functions are the necessary data from which the control source filters are derived.

The system was tested by pre-convolving the audio signals. A real-time implementation of the filtering was tested in a later experiment using the same experimental setup.

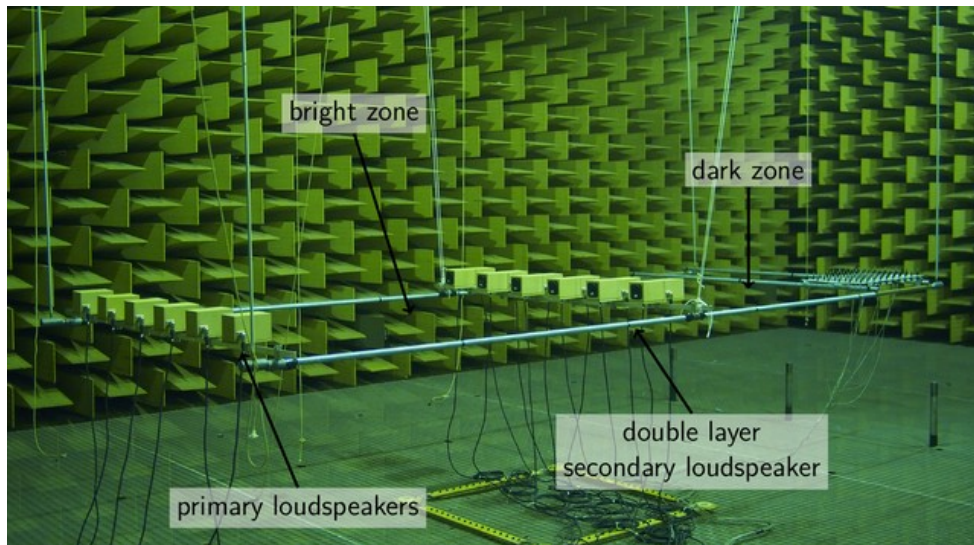


Figure 12: Photo of small scale anechoic experiment setup

3.5.2.2 Results and Discussion

We quantify the performance of the sound field control method in terms of insertion loss and primary to secondary ratio. We define the insertion as the mean change in sound pressure level in the dark zone when comparing the sound field with active and deactivated control sources. A high insertion loss indicates a large reduction in sound pressure level. For the bright zone, we define the primary to the secondary ratio as the ratio of ratio of mean sound energy from the primary source to the secondary sources. A large ratio indicates that most of the sound energy is due to the primary source, suggesting that the secondary sources are not audible in the audience area.

Figure 13 shows both quantities for the anechoic setup. We observe an insertion loss of about 10 dB up to around 1 kHz (which is equivalent to 100 ~ 200 Hz in full scale setup), after which it drops quickly. The primary to secondary ratio is larger than 18 dB in that frequency range, showing that the double layer array is directing most of the radiated sound energy to the dark zone. In fact, noticing the secondary sources in the bright zone during music playback was, if at all, only possible very close to the control sources.

Figure 13 compares the spatial distribution of the sound pressure level for the controlled and uncontrolled case for three frequencies. The SPL reduction is especially strong in the left half of the dark zone. This patch of strong reduction is getting smaller with frequency. However, it is also present above the Nyquist frequency of around 570 Hz of the line arrays. The setup here is representing a worst-case situation where the dark zone is just behind the control sources. In general, one can expect the Insertion Loss (IL) to increase with the distance between the dark zone and control loudspeakers because at large distances the decays of sound from primary and secondary sources get more similar.

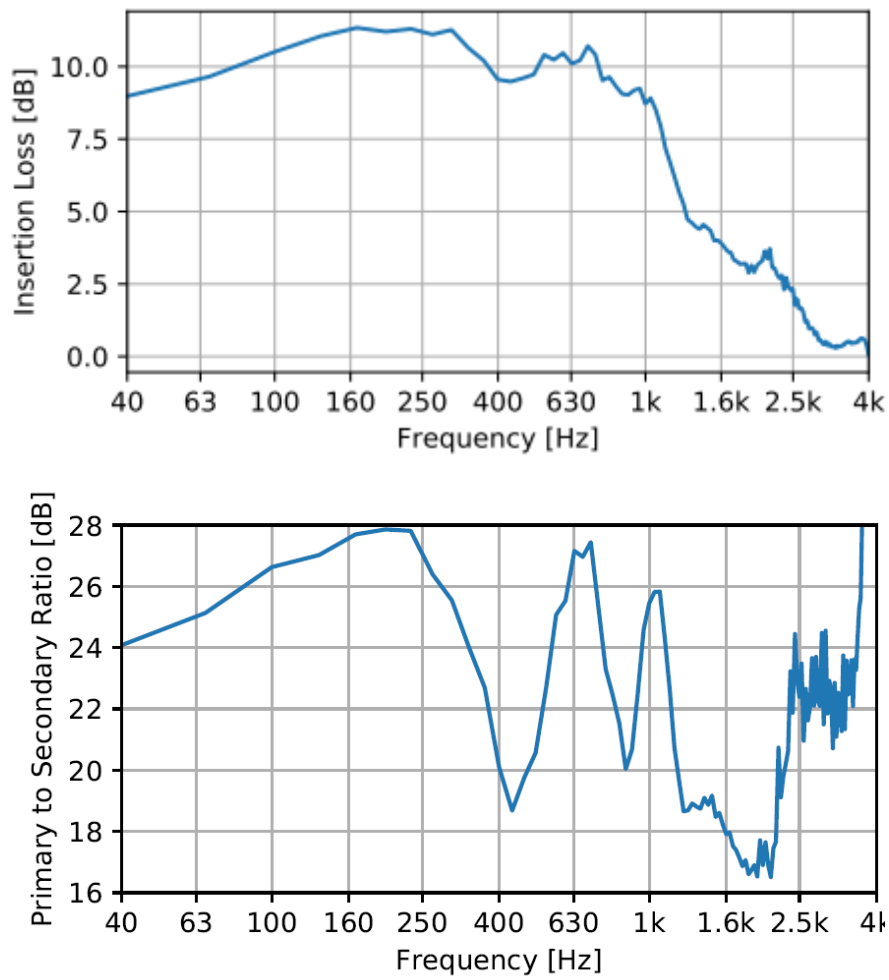


Figure 13: (Top) Insertion loss (IL) of sound field control system in anechoic experiment. Higher values indicate a larger reduction of sound pressure level in the dark zone. (Bottom) primary to secondary ratio in anechoic experiment. Higher values indicate less distortion by control loudspeakers in bright zone.

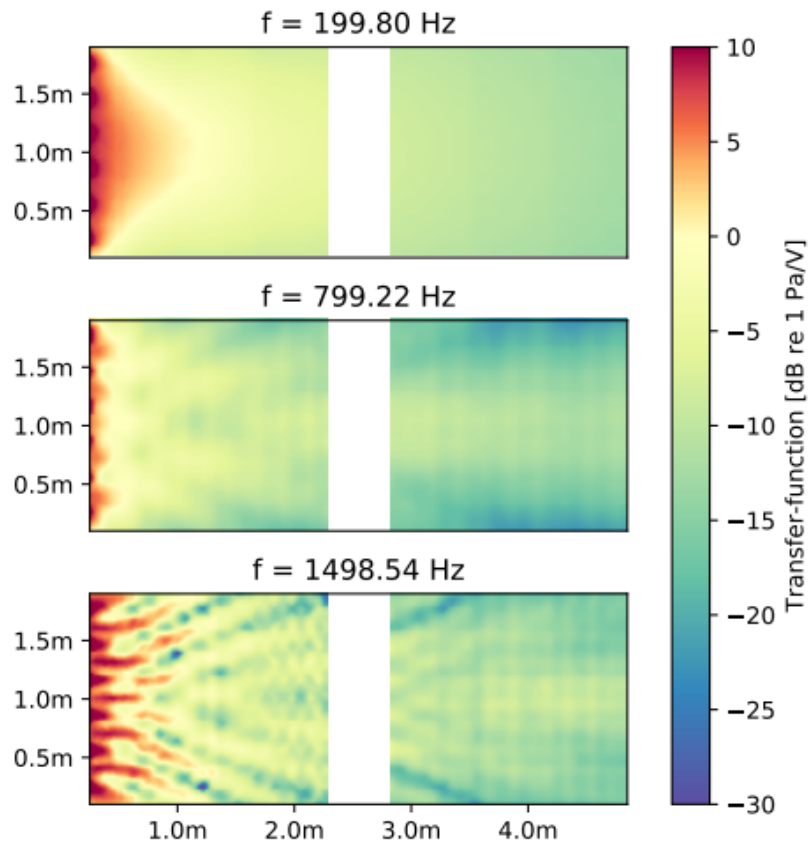


Figure 14: No control: magnitude of sound field in bright (left) and dark zone (right) at three frequencies. Primary sources are at $x=0$. The secondary sources in between the two zones.

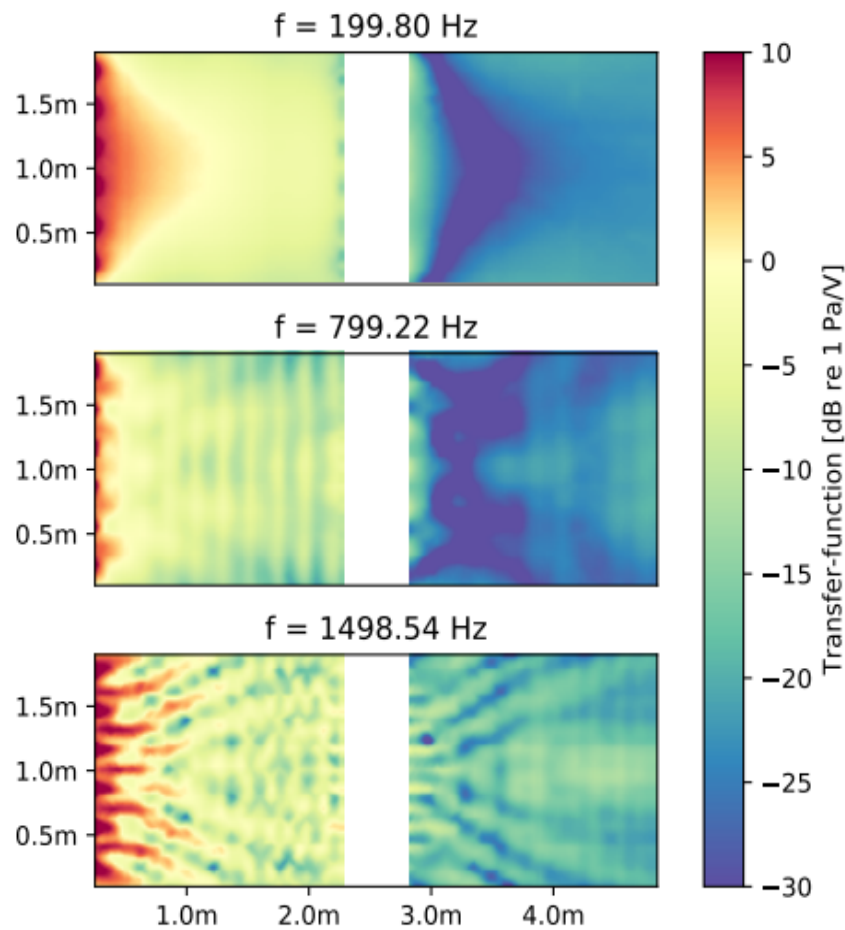


Figure 15: With control: magnitude of sound field in bright (left) and dark zone (right) at three frequencies. Primary sources are at $x=0$. The secondary sources are in between the two zones.

3.5.2.3 Conclusions

We experimentally verified that the sound zone approach can actively reduce sound pressure levels in a dark zone without significantly disturbing the sound experience in the bright zone. The test was undertaken in anechoic conditions and with pre-convolved sounds, i.e. not in real time. We also tested and verified our methods for measuring the necessary transfer functions.

To test the system under more realistic conditions, we conducted the next experiment.

3.5.3 Large scale outdoor experiment

In May 2018 a full scale test with professional PA equipment was conducted at Refshaleøen in Copenhagen. The goal of this experiment was to investigate and test the sound zone system in a more realistic setting. At the same time, we wanted to get familiar with integrating the system with professional sound reinforcement equipment. In comparison to the anechoic chamber measurement, there were reflections from the ground and from a few objects scattered around the area, varying temperatures, larger control zones, more loudspeakers, loudspeakers with cardioid radiation pattern, and a lower frequency range.



Figure 16: Photo of large scale outdoor experiment setup. The experiment took place at Refshaleøen in Copenhagen, a former industrial area.

3.5.3.1 Experimental setup

Figure 16 shows a photo of the experimental setup, which spanned a region of 80 m × 20 m. The primary sources comprised 10 subwoofers arranged in a line array with 2 m spacing. The secondary sources consisted of 20 subwoofers of the same type arranged in a double layer line array. The subwoofer model had an intrinsic cardioid radiation pattern and a nominal frequency range of 37 – 115 Hz (-5dB). If a single layer of cardioid speakers creates enough primary to secondary ratio there is no need for a double layer arrangement and the number of loudspeakers could be reduced by a factor 2. The transfer-functions to the bright and dark zones were sampled at 100 microphone positions in each zone, half of which was used for the computation of the control filters and the other half for the performance estimation.

3.5.3.2 Results and Discussion

Figure 17 shows the performance metrics of the sound field control solution. We estimated a maximal insertion loss of around 12-14 dB between 45-85 Hz when using either two (blue continuous) just one layer (yellow dashed) of secondary sources. Using a double layer does not significantly increase the insertion loss but increases the primary-to-secondary ratio by 2-10dB. The primary to secondary ratio is larger than 15 dB at all frequencies for both cases, suggesting that a single layer of cardioid secondary sources could be focusing its sound energy sufficiently well away from the bright zone.

We measured the transfer-functions of all single sources for computation of the filters and prediction of the results at noon in peak temperatures. We also directly measured the sound field of the total system at the beginning of the night, when temperatures had fallen by 6-8 °C (green dash-dotted). The change in weather conditions resulted in a change of the speed of sound and thus changed the transfer-functions. This mismatch in conditions during transfer-function measurement and playback lead to a reduction of the insertion loss by 2-10 dB (see discussion).

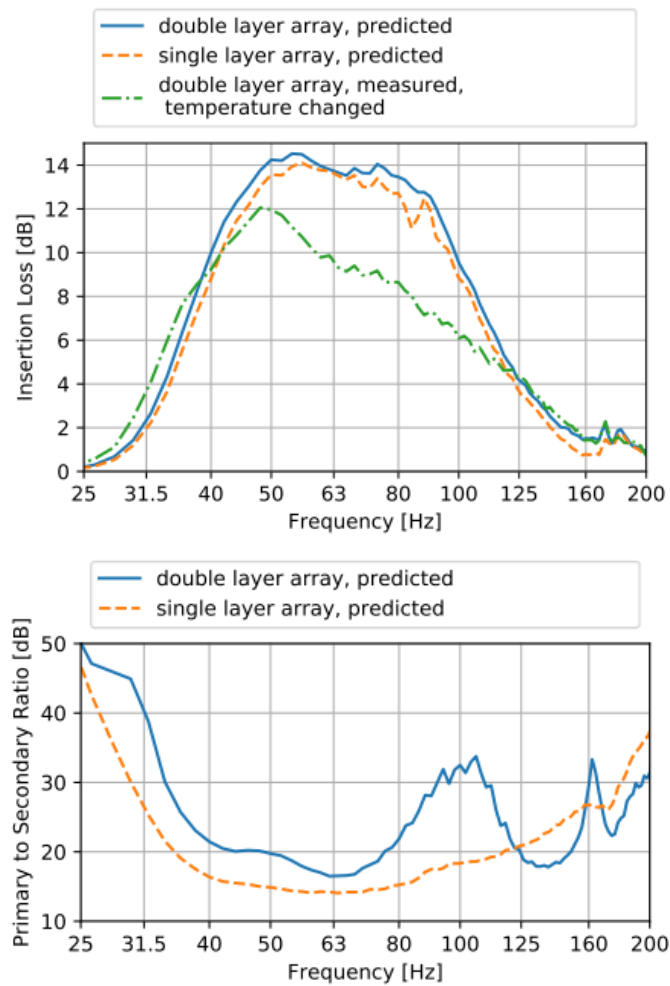


Figure 17: Performance metrics at outdoor experiment. (Top) insertion loss. (Bottom) primary to secondary ratio.

3.5.3.3 Conclusions

We could successfully validate the concept of the sound field control system in a geometrically simple environment (flat ground only). Instead of using a double layer of control loudspeakers and explicitly taking the bright zone in the optimization into account, we observed that a single layer of cardioid secondary sources might be sufficient in directing sound energy from the control sources away from the bright zone. While we have not investigated the impact of changing environmental conditions thoroughly, we could observe that changes in temperature can have a significant impact on the performance of the control system.

3.5.4 Pilot Test: Kappa Futur Festival 2018 (KFF2018)

In the largest of the three experiments, the sound field control system was put to test during the Kappa Futur Festival 2018 (KFF2018). Compared to the previous experiments this scenario posed several new challenges: complex, uneven terrain with many reflecting structures and surfaces around the venue and dark zone, i.e. late reverberant reflections which cannot be captured in a short FIR filter; microphone positions neither in line of sight with the primary source nor the secondary sources, i.e. indirect sound must be canceled by the indirect sound from the secondary sources; restrictions in placement of secondary sources and microphones, i.e. fewer samples of the transfer-functions to the dark zone; and time constrained measurements in noisy environment at large distances, i.e. low signal to noise ratio in transfer-function measurements. Here we also computed the control loudspeaker signals in real time.



Figure 18: Kappa Futur Festival



Figure 19: Control subwoofer at Kappa Futur Festival 2018. The festival stage can be seen in the back.

3.5.4.1 Experimental Setup

Figure 19 gives an overview of the venue, the setup of loudspeakers and the microphone positions in and around a part of the festival area that spans around 300 m. The primary source (main stage subwoofer system) comprised 20 cardioid subwoofers in a digitally curved line array configuration. The secondary source array consisted out of 16 subwoofers of the same type arranged in a single line with 2.55 m spacing (center-center) and facing the negative x-direction. The stage sound system also featured two vertical line arrays for the higher frequencies, but these were not included in the transfer-function measurements and thus also not accounted for by the sound field control system. We assumed that the secondary source configuration and the large distance of the secondary sources to the audience area would lead to a low impact of the control system onto the audience area, which was approximately the area between $x = 100$ m and $x = 200$ m. In fact, a difference from switching the control speakers on and off could only be noticed up to around $x = 90$ m. Closer to the audience area the sound from the secondary sources was completely masked by the sound from the primary source.

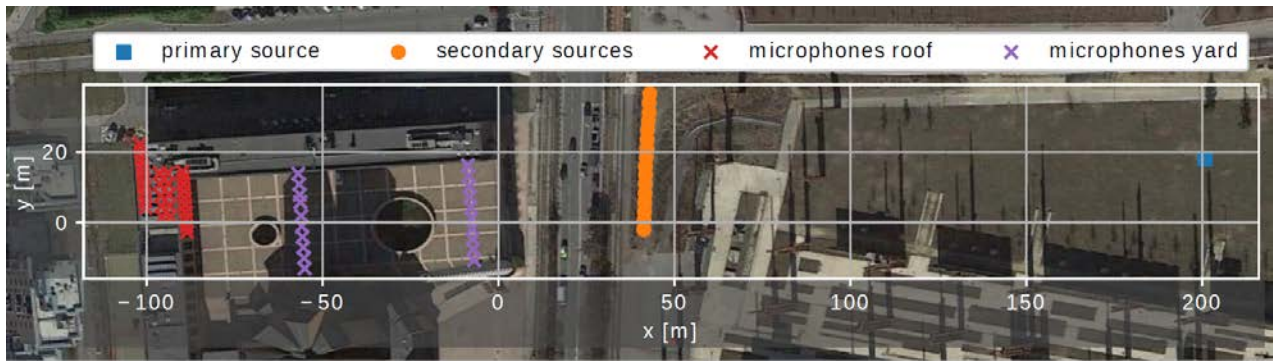


Figure 20: Arrangement of control sources and microphones at Kappa Futur Festival 2018

The dark zone was defined as the area between $x = -100$ m and $x = 0$ m. It was sampled at 20 microphone positions in an elevated courtyard and 30 positions on a rooftop. After measurement of the transfer-functions from all sources to all microphone positions, a set of control filters was computed, and the regularization parameter was chosen by hand such that the gain of the control filters was not overly extreme.

3.5.4.2 Results and Discussion

Figure 20 shows the measured magnitude response of the sound system with active and disabled secondary sources at the line of microphone positions around $x = -10$ m and compares them to the prediction. They align well, showing an IL up to about 6 dB. If we can use the prediction also for all other positions, we estimated the average IL at all microphone positions by offline prediction in Figure 20.

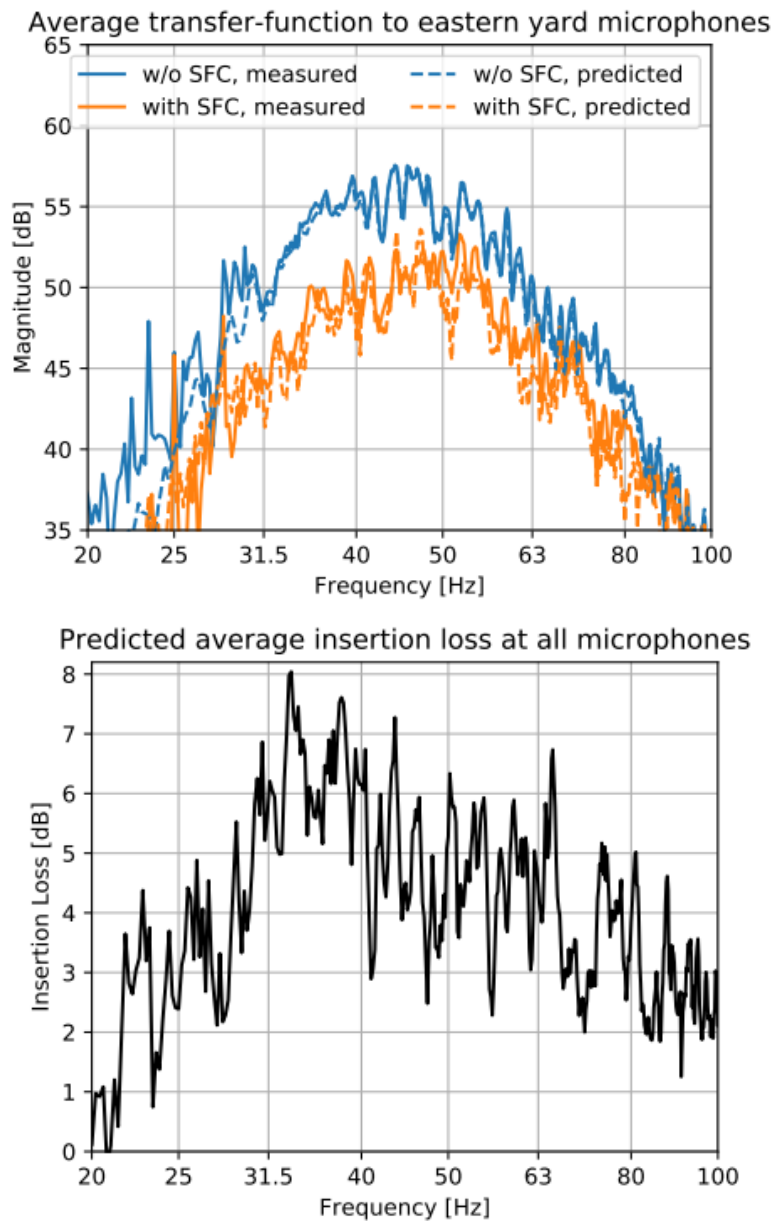


Figure 21: Performance at Kappa Futur Festival 2018.

3.5.4.3 Conclusion

The sound field control system was successfully tested under live conditions. However, the reduction of sound pressure level is below the set target of 10 dB in the low frequencies. The reasons for this result is most likely related (but to a lower degree) to the problems that occurred during the Tivoli pilot, reported next.

3.5.5 Pilot Test: Fredagsrock (Tivoli2018)



Figure 22: Control array at Tivoli 2018 pilot.
The courtyard of the building in the background was used as the dark zone.

The sound field control system was also deployed at a second pilot test at a concert at Tivoli. We faced several new challenges here, which all together lead to an unsuccessful test:

- We had problems during measurement of transfer-functions
 - Desynchronization of recording front ends connected to microphones and signal generators. The measurements of the transfer functions were not aligned in time properly which makes it impossible to calculate the cancellation filter. Only a subset of the measurements could be used.
 - Continuous rain during transfer-function measurements during Thursday when the measurements were planned.
- Change in conditions between measurement of transfer functions and concert time.
 - Atmospheric conditions changed and the system was not defined to be adaptive yet.
 - The effect of the audience in the sound propagated from the primary sources.
- Strongly reverberant sound field in dark zone as the microphones were placed in a court yard in front of the park.
- We had to adapt to the setup implementing a new dual channel control, as the subwoofer system was driven by two separate audio channels. It had to be designed ad-hoc without proper previous validation.
- We worked with a different brand (LAcoustics) which gain reduction pre-sets are not well known by us.
- Most of the low frequency range (down to 65 Hz) was also produced by the hanging top loudspeakers. This led to a more complex configuration.
- The signal to noise ratio is very low because there is a main road very transited in between the park and the measurement place, increasing the background noise. In addition the music signal was low compared to the level we could reach in Torino.

No results from Tivoli is presented here, as the measurements showed no effect or Insertion Loss of the system.

3.6 Future work

In 2018 we could prove the principle of reducing sound actively with sound field control. In 2019, we plan to refine our methods to enhance the effect of the ASFCS and improve the reliability of the system to avoid technical problems.

The main topics will be:

- Adapting sound field control system to changes in atmospheric conditions (e.g. temperature)
- Integration of ASFCS with IoT microphones and the MONICA cloud
- Improving measurement and tuning procedures

We are planning at least three experiments in 2019: a controlled test in May and tests at Kappa Futur Festival and Tivoli Fredegsrock.

4 Quiet Zones – near field control (T4.1.2)

4.1 Technology overview

The Quiet Zone (QZ) system is a noise barrier which makes use of active elements to cancel out low frequencies and passive elements to block high-frequency noise. The goal is here to obtain the highest possible attenuation of noise across the whole listening spectrum. The system is integrated into the ASFC environment and provides local quiet zones within or close to the optimized sound-field of the ASFC system without interference. The QZ system is based on (traditional) active noise control.

The active part of the QZ system consists of arrays of loudspeakers which synthesize the canceling sound-field to cancel out the noise-field in the desired zone. Such multichannel active noise canceling methods in free-fields are described (Kuo, 1996) and (Hansen and Snyder, 2002). The active noise canceling principle is nowadays well known from appropriate headphones which have entered the consumer markets. Of special challenge in the MONICA project is that we have to cope with distributed noise sources which reach the quiet zone areas from different angles and are transmitted through varying paths due to changing conditions (wind, temperature, moving people). The task is to cancel out sound under free-field conditions, with sparse, random and broadband noise sources (the music signal coming from the many distributed loudspeakers of the venue). Figure 22 shows an open-air concert area with ASFC and quiet zones.

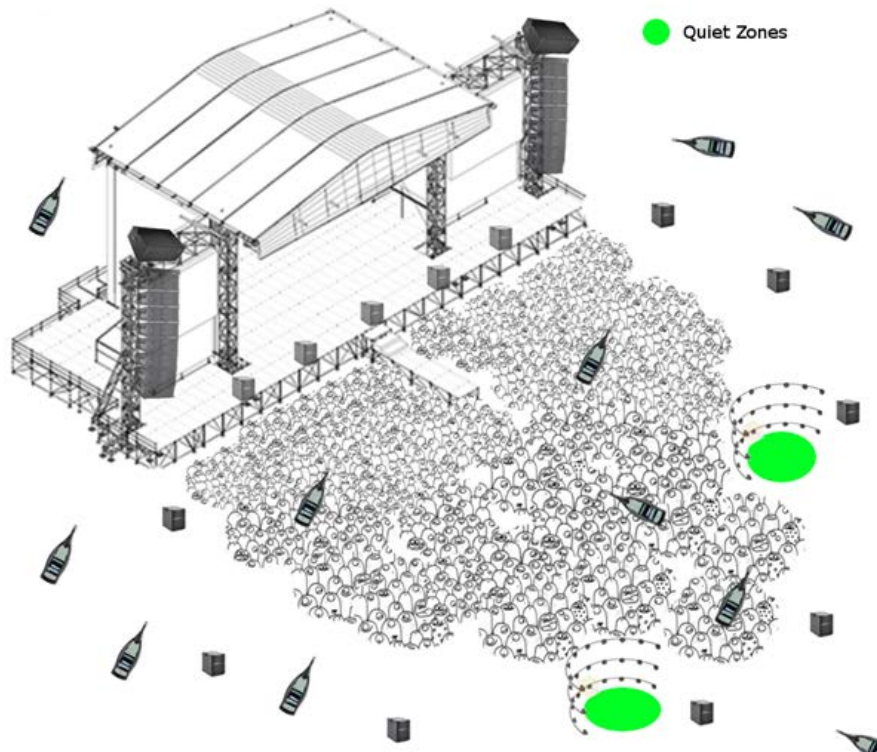


Figure 23: A possible use case of quiet zone systems in a loud outdoor venue

Figure 23 shows the prototype of the quiet zone system. It has been constructed and tested in the *Fredagsrock* Concert at the pilot venue Tivoli. The quiet zone area is about 2 m x 1 m x 0.6 m (w/d/h) and should be able to accommodate at least two persons trying to communicate verbally.



Figure 24: Prototype of the Quiet Zone System tested at the Tivoli pilot site. The controller and the error microphones are not shown here.

The active part of the system makes use of a multichannel filtered reference signal least mean square algorithm (MC FxLMS). Based on simulation a practical/optimal number of 4 microphones and 4 secondary loudspeakers have been chosen. The microphones measure the sound pressure in their individual positions and feed the algorithm, which finds the optimal set of filters to cancel the sound in the error microphone positions as best as possible. Changes in the electro-acoustical conditions will be reflected, which means that the system adapts automatically to these and changes the filter coefficients accordingly. Figure 24 shows such a multichannel controller architecture.

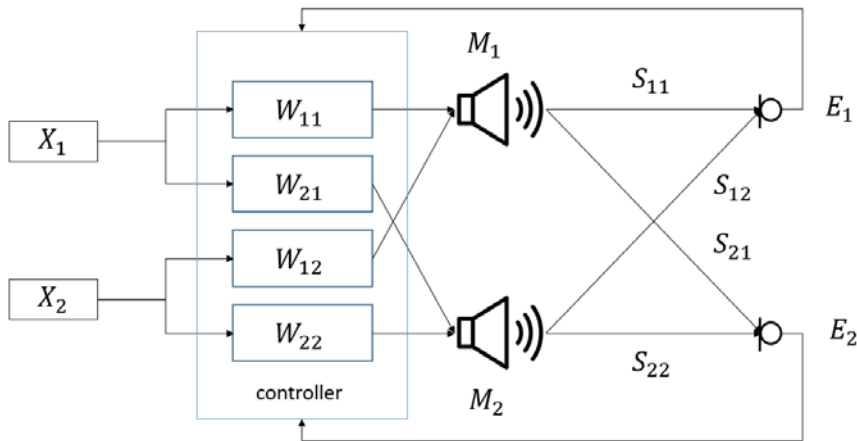


Figure 25: Multichannel Controller Architecture. X: Reference signal (from mixing engineers console), W_{ii} FIR filters, M_i Secondary loudspeakers, S_{ii} sound propagation paths, E_i : Error measurement positions.

The passive element has a double purpose. It acts as a noise barrier and blocks high frequencies from the quiet zone. On the other hand, it is the housing for the four subwoofers and provides the volume, which is needed to keep the resonance frequency of the loudspeaker low in order to get a flat response down to ca. 35 Hz.

The overall technical system consists of standard professional audio equipment, see Figure 25.

- 1x 4 channel amplifier

- 4x subwoofers
- 1x Multichannel Audio Interface: RME Octamic
- 4x B&K free-field microphones + signal conditioner
- 1x Computer running the ANC software in MATLAB

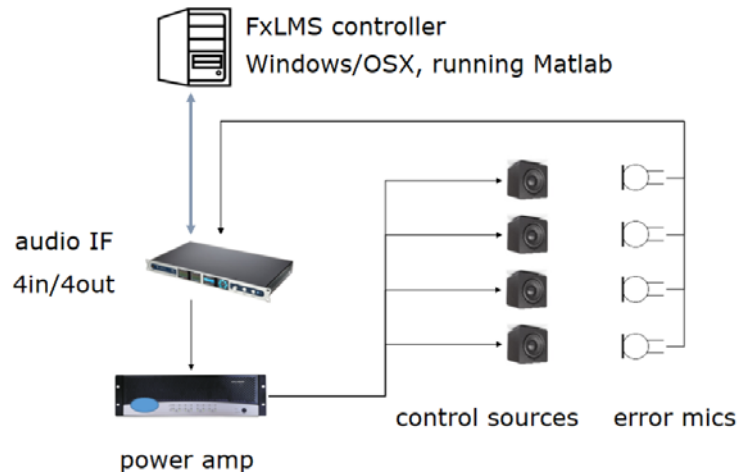


Figure 26 Technical Architecture of the Quiet Zone system (active part).

4.2 Services enabled

The quiet zones are related to the use case "Sound Level Adjustment" and the solution "Sound Control".

4.3 Infrastructure and integration with the MONICA IoT platform

The position of the quiet zone systems will be displayed in the COP (Common Operational Picture); this was implemented in the 2018 Tivoli test.

4.3.1 Audio Signals from the Venue

The quiet zone system receives the audio signals from the venue's console or from behind the PA's power amplifiers. The latter would be the primary choice because the standard PA system incorporates signal processing units into the power amplification stage. For example, devices such as Limiters cause nonlinear components which will decrease the performance of the active noise controller.

4.3.2 Operational Status

Figure 26 shows a link to the propagation model unit. This link is used as a "through" port to the MONICA cloud only but provides the possibility for further optimizations of the ASFC and QZ system, such that the local and far-field transfer-functions could be exchanged for example.

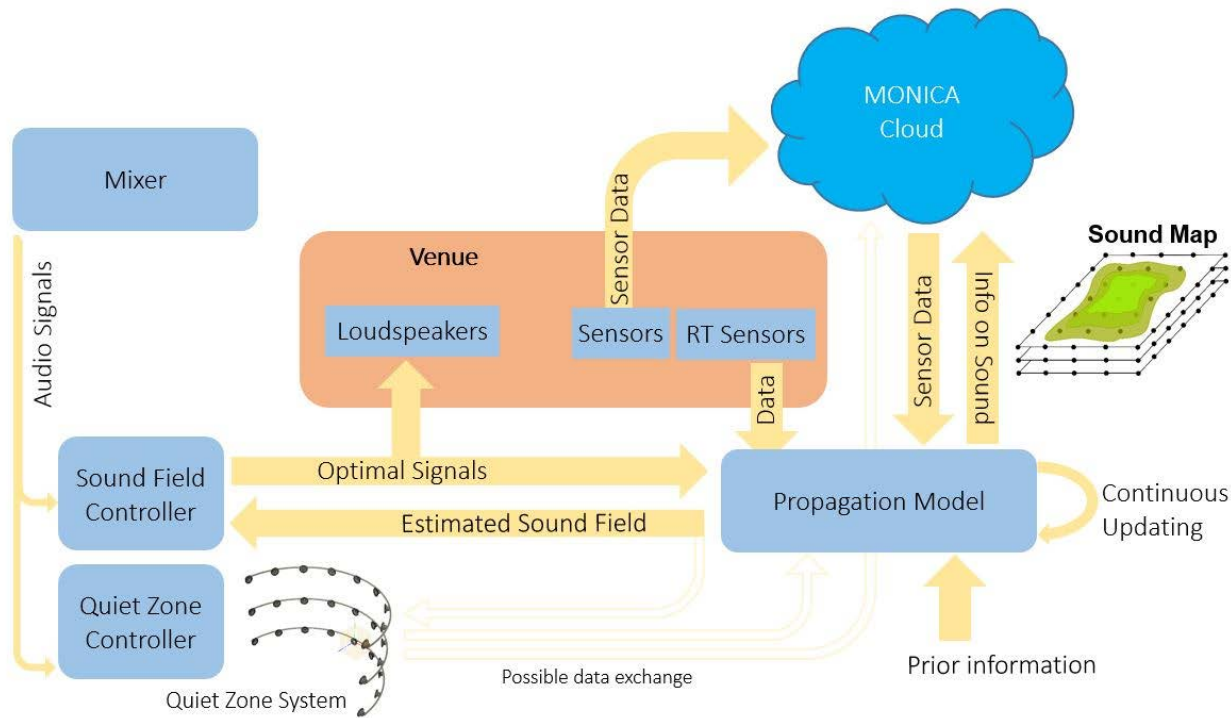


Figure 27: Information flow chart, ASFC including the Quiet Zone.

4.4 Simulation

Simulations have been carried out to estimate the optimal performance under practical constraints. These simulations led to the configuration of 4 control sources and error microphones, which has been used in measurements to evaluate the theory and was finally tested at the Tivoli pilot site. Figure 27 shows the results of simulations using a band-passed pink noise signal (100-300 Hz) as a reference signal (which represents the music from the venue's PA). What we see is that the closer we come to the microphone array, the larger is the insertion loss, which makes sense because the optimization routine tries to reduce the pressure in the error microphone positions. What also can be seen is that there is still promising attenuation in the close vicinity of the error microphones – the quiet zone area.

4.5 Measurements

The results from simulations have been verified by measurements in an anechoic chamber. The setup has been arranged according to the arrangement in the simulations. Figure 28 shows the results measured with a 60 channel microphone from B&K in the quiet zone. This array was moved 4 times in order to measure 240 positions. It can be seen that the measured insertion loss is quite congruent with the simulations. Furthermore, the vertical extension of the zone has been measured and it can be seen that up to 30 cm below and above the microphone array is still a reduction of about 10 dB, see Figure 29. Finally, we can say that with 4 secondary sources and microphones it is possible to produce a volume of silence with ca. 13 dB average attenuation in the dimensions 2m times 0.75m times 0.6m (width/depth/height).

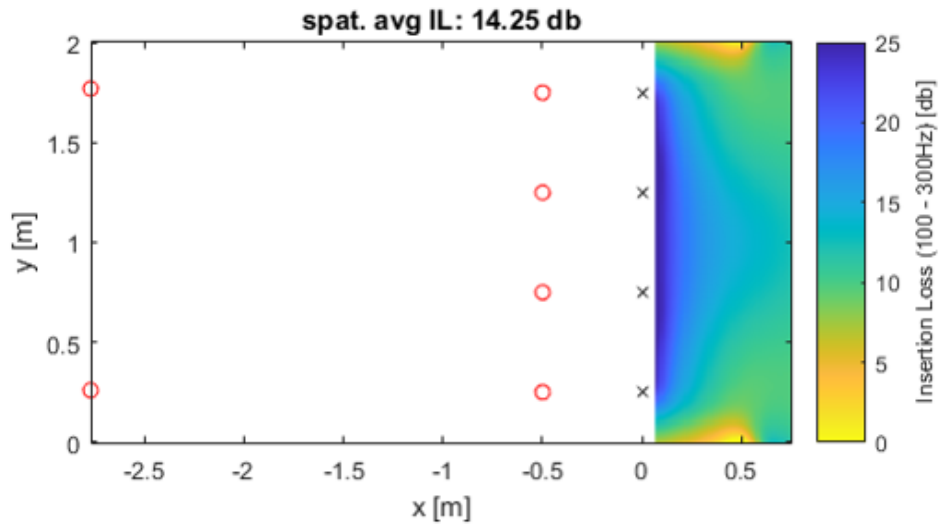


Figure 28: Results from Simulations. This plot shows the Insertion loss in the quiet zone (colored area). Red circles on the left: the venue loudspeakers, red circles in the middle: control speakers, black crosses: error microphones. The insertion los averaged over the whole zone is 14.25 dB.

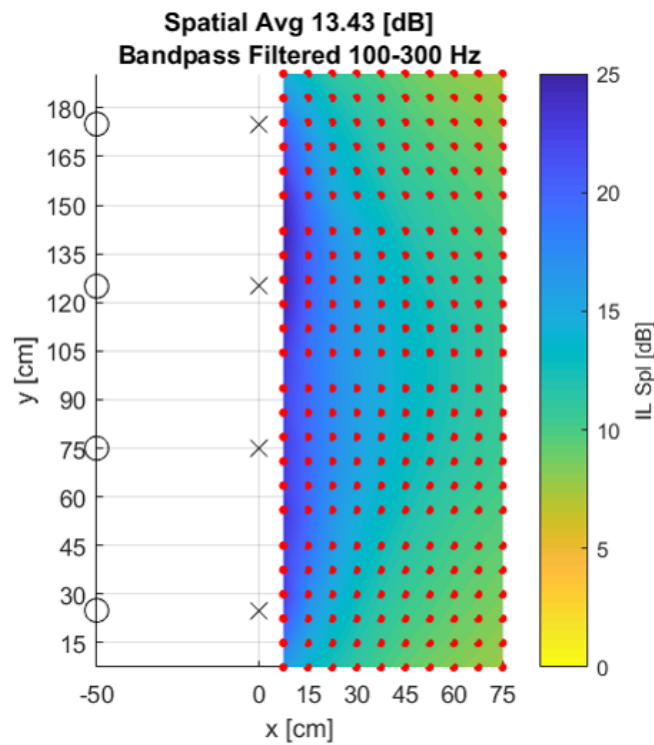


Figure 29: Measured Insertion Loss in Quiet Zone, red dots: measurement positions, black circles: control sources, black crosses: error microphones

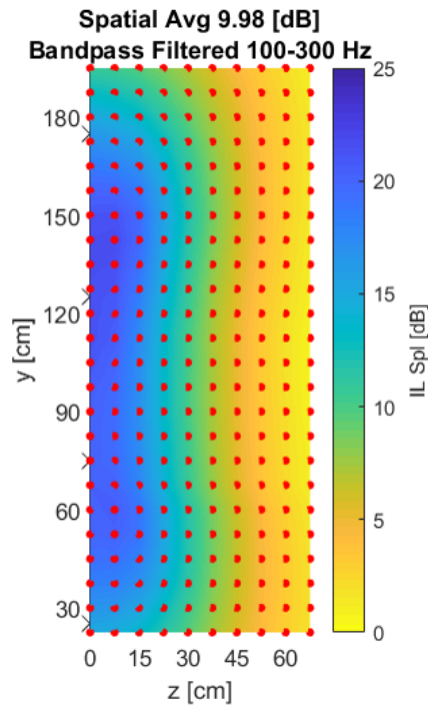


Figure 30: Vertically measured Insertion Loss, up to 10 dB attenuation 30cm above the microphone array

4.6 Pilot Test at Tivoli

Finally, we have constructed the complete system and tested at the Tivoli pilot site. In this case, the reference signal was the music from the band MEW coming directly from the console. The challenge here was that the algorithm had to cope with non-stationary signals and very long filters due to reflections on distant surfaces. For the evaluation, it had been chosen to compare the transfer-functions between

$$\frac{Error\ Mic}{Reference} \text{ to } \frac{Ref\ Mic}{Reference}$$

The Reference Microphone has been placed about 3 m away from the quiet zone, the Error Microphone was at the front edge of the quiet zone, off-centered with 25 cm. Figure 30 shows the two curves gained from 20 seconds average.

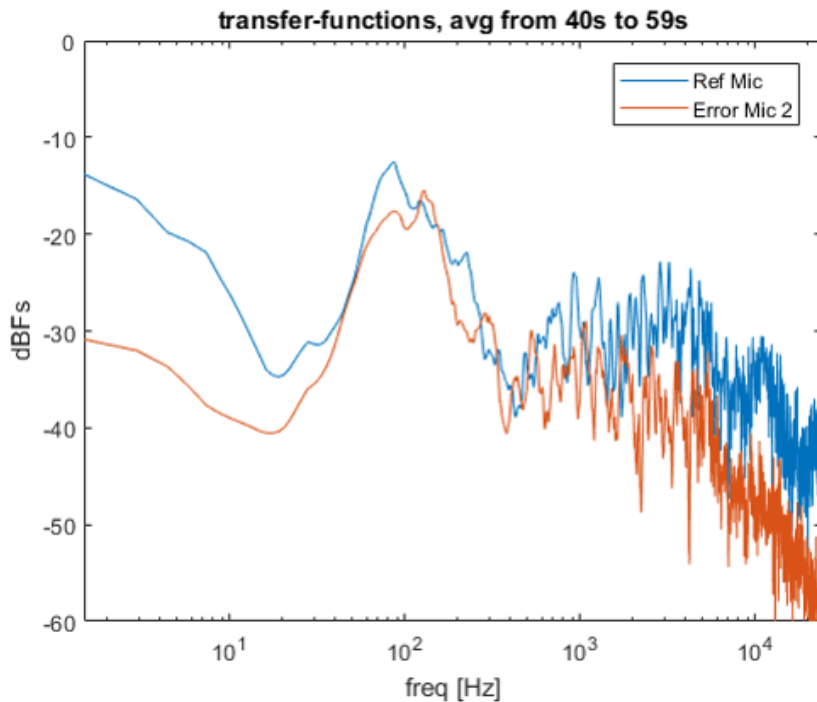


Figure 31: Extracted transfer functions from an Error Mic and a Reference Mic.

It can be seen that there is no attenuation for frequencies in the low end (30-300 Hz) and increasing attenuation for higher frequencies. The active controller did obviously not work, the passive as expected on the other hand. The evaluation of the system failure had been moved to a later point and is not further covered in this report.

Possible reasons for the failure or at least for performance reduction are:

- The non-stationary character of the reference signals could have caused problems, especially the fact that music correlates with itself.

The length of the adaptive filters had to be kept at a certain limit in order to limit the computational effort. Therefore some parts of the distant reflections haven't been accounted for. Unaccounted reflections of the noise decrease the performance of the system.

4.7 Future Work

The system failure is analyzed at the end of 2018. In the following month will new algorithms of active control be investigated with the goal to either increase the insertion loss or to reduce the computational effort. Also, the robustness against disturbance and the non-stationary character of the reference signal is still under investigation.

5 Sound zone signal processing and optimization (T4.1.3 and T4.3)

5.1 Technology Overview

5.1.1 Sound Zone Signal Processing

Sound zone signal processing and optimization scheme in ASFCS is based on the combined solution of Pressure Matching and Acoustic Contrast Control (PM-ACC) proposed in (Chang and Jacobsen, 2012). PM-ACC is a technique that can select a hybrid solution between the pure contrast solution (ACC) (Choi and Kim, 2002) and the pure pressure matching solution (PM). The solution aims to minimize the pressure field error in the bright zone while keeping the acoustical potential energy low in the dark zone (the neighboring region). PM-ACC solution fits well for the objective of the project because the sound field control in the dark zone must not negatively affect the sound quality and music experience in the audience area.

In parallel with the large-scale outdoor experiment (section 3.5.2), we have conducted an informal listening test to see the effect of a secondary array to the sound quality in the listening area. Total 21 subjects spread out in the listening area and tested whether they can discriminate the sound difference when the secondary array is turned on. However, all 21 subjects failed to discriminate the sound difference and only possible to perceive the difference when the subject is very close to the secondary array less than two meters. It means that we can ignore the sound quality degradation due to the secondary array. Therefore, PM-ACC solution that we use is modified in order to maximize the Acoustic Contrast and the pressure field error is not seriously considered.

Figure 31 shows the process of obtaining the solution. The zones (bright and dark) are selected considering the condition of venue and the neighboring region. Transfer-function data and *desired target field*⁶ in the bright zone are needed for calculating the optimal solution. The optimal solution applies to FIR filter coefficients for the input signals to secondary sources. The input signal to each secondary source is coherent with the monitored input signal that fed into the primary sources.

The optimal solution of PM-ACC is explicitly given in (Chang and Jacobsen, 2013). Since the solution is given explicitly, no additional optimization process is needed for the calculation. However, the solution needs a matrix inversion process which requires regularization methods for obtaining a robust solution. The matrix involved in the inversion process is a positive semidefinite matrix, where the inversion of the matrix can make the system sensitive to the transfer-function error estimated from the Sound Propagation Model. To avoid this situation, various regularization techniques or additional constraints can be applied. In this case, the solution may require a different optimization process.

⁶ The target field is the desired sound field in the audience area. For example, this can be the propagating wavefield from sources in the position of the PA loudspeakers, without disturbing reflections and artefacts.

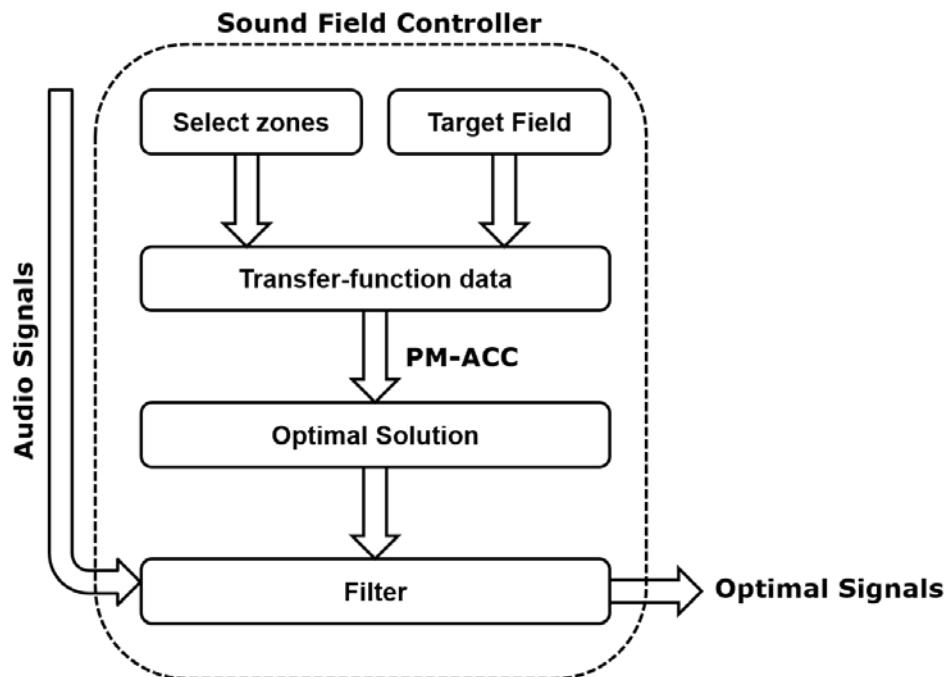


Figure 32: Signal processing flow of the Sound Field Controller, which is a module shown in Figure 2.

5.1.2 Sound Propagation Model

Sound field control in outdoor concerts requires accurate estimates of the transfer functions between sources and receivers. Feedforward approaches are based on direct measurements of the transfer functions in a dense grid of points. This makes them intractable for large-scale situations like the ones present in this project, showing the need of propagation models in order to characterize the sound field in such large areas and provide the ASFCS the proper transfer functions. During the first year, we investigated the adequateness of *Nord2000* as a proper propagation model for outdoor sound field control, presenting severe limitations when modeling sound propagation at low frequencies. It implied the research and development of alternatives.

A new model based on spherical harmonics has been successfully tested under controlled conditions in the anechoic chamber for a scaled setup of 2 x 5 m. The acoustic contrast produced when using this model is very similar to the one we would get using a dense grid of microphones. Figure 32 shows a comparison of the insertion loss for such setup between measuring transfer functions at 1400 microphone positions and measuring only at 16 sparse microphone positions using the model (Figure 33).

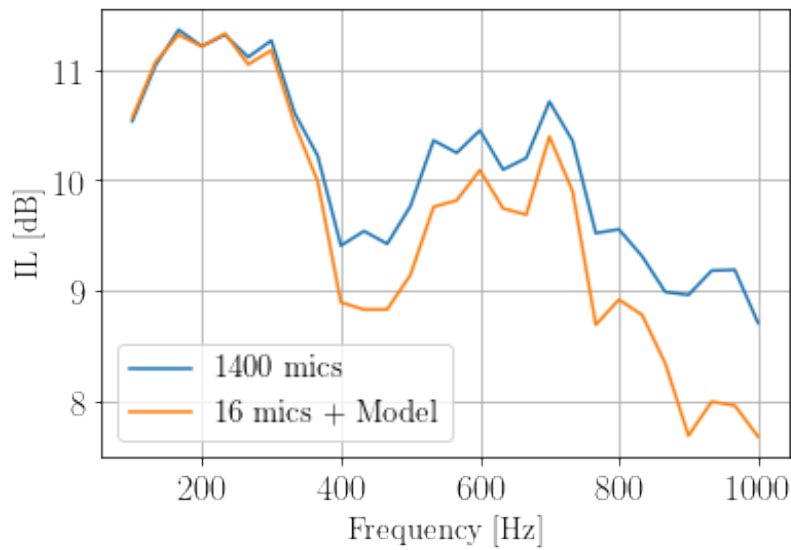


Figure 33: IL comparison between using 1400 microphones and 16 microphones with the spherical harmonics model.

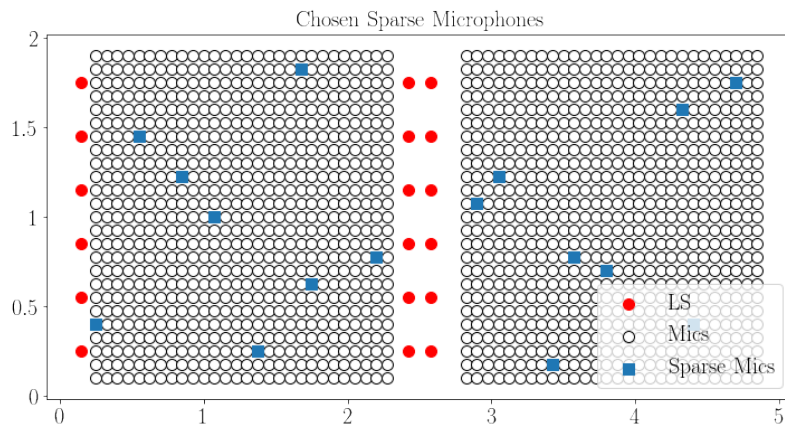


Figure 34: Setup with 1400 microphones (white) and 18 loudspeakers (red). In blue the 16 microphones to fit the model and reconstruct the transfer functions.

Machine learning techniques are used to fit the parameters of the model according to the sparse measured data and deal with the uncertainties present in the parameters, leading to a good performance of the sound field control strategy. In (Caviedes and Brunskog 2018) we showed how machine learning techniques can be used in fitting models for sound field control problems.

These uncertainties come from different causes such as atmospheric variations, error in the measurements and noise. Thanks to the IoT network deployment present in MONICA we can gather the data to fit our propagation model. Data from weather and acoustic sensors can be continuously stored and used, and the propagation model can be continuously updated accounting for weather conditions, change in the crowd distribution and other causes that may affect how the sound propagates during a concert. In Section 5.5 we show results from a measurement campaign in order to quantify the effect of atmospheric conditions in the measured transfer functions. This is another step towards defining a model that properly describes the outdoor sound propagation.

5.2 Services enabled

Signal processing and optimization algorithm is embedded in ASFCS computational core. See further in section 3.2

5.3 Infrastructure and integration with the MONICA IoT platform

The sound zone signal processing and sound propagation model are running on the processing unit as described in section 3.3.

5.4 Simulations

In this section, simulations are present on how the sound propagation model is updated with machine learning and used together with the ASFCS (See section 3.4 for ASFCS detailed simulations). A simplified version of the simulations in section 3.4 was specified in (Heuchel and Caviedes, 2017) and can be seen in Figure 34. The bright zone is bounded by two loudspeaker arrays with 5 and 10 loudspeakers, respectively. The target field in the bright zone is a 100dB SPL plane wave traveling in the negative y-direction. The dark zone is placed 17.5m away from the bright zone. Both zones are sampled at 2.5 evaluation points per maximum wavelength in each direction. The frequency range of interest is from 20 to 250Hz with a frequency resolution of 15.33Hz. Both evaluation points and loudspeakers are positioned 1.6m above the ground. The ground is again considered compacted park area (Impedance Class E according to Nordtest) with $\sigma = 700 \text{ kPa} \cdot \text{m/s}$ (see Plovsing,2000). The speed of sound is $c = 343 \text{ m/s}$ and air density $\rho = 1.2 \text{ kg/m}^3$. The loudspeakers are modeled as monopoles with constant magnitude response. The dark zone mean-square pressure is bounded to be less than 60 dB SPL. The regularization parameter was chosen $E0 = 50\text{m}6\text{s}-3$, as it leads reasonable solutions for this problem.

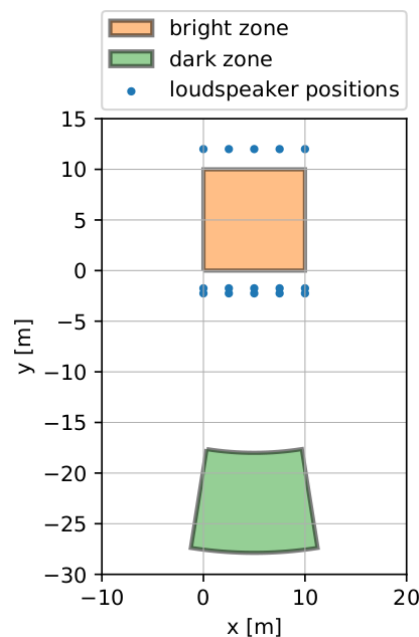


Figure 35: Setup of bright zone, dark zone and fixed loudspeaker positions in the simulation.

In order to resemble real conditions in the simulations, measurement noise and uncertainties need to be generated for the desired parameters. Measured coordinates of both sources and receivers are affected by 15 cm of random deviation. The measured pressure is distorted with 30dB SNR for all the frequencies. The ground is considered park area, so the flow resistivity is set as the representative value of the Impedance Class E in Nordtest ($500 \text{ kPa} \cdot \text{m/s}$). A summary of the parameters is presented in the following Table 2.

| Parameter | | Value |
|-----------|----------------------------------|-------------------------------------|
| D_0 | Max. Mean squared pressure in DZ | $20 \mu\text{Pa} \times 10^{60/10}$ |
| E_0 | Regularization parameter | $50 \text{ m}^6\text{s}^{-3}$ |
| SNR | Signal to Noise Ratio | 30 dB |
| - | Coordinates Error | 15 cm |
| σ | True Flow Resistivity | $700 \text{ kPa} \cdot \text{m/s}$ |
| σ' | Forward Flow Resistivity | $500 \text{ kPa} \cdot \text{m/s}$ |

Table 2: Nord2000 model parameters

Figure 35 shows the Acoustic Contrast (AC) with and without ASFCs in the cases of true parameters, forward parameters, and optimized parameters. No sound field control describes the case where only the upper loudspeaker array is active with constant source strengths. That contrast is only due to the distance of the zones to the sources (what cases like *Kappa Futur Festival* and *Tivoli Fredagsrock* are experiencing). Applying the sound field control system improves the acoustic contrast by 17 dB-35 dB in the ideal case of true parameters. If the forward parameters are used without model updating/machine learning techniques, the acoustic contrast drops down to 10 dB, even though the uncertainty in the positions is small compared to the wavelength. This is the case of using directly an engineering sound propagation model such as *Nord2000*. Using model updating/machine learning to optimize, the contrast enhances the improvement again, especially at low frequencies; a benefit of about 10 dB is seen in Figure 35 for the low frequencies.

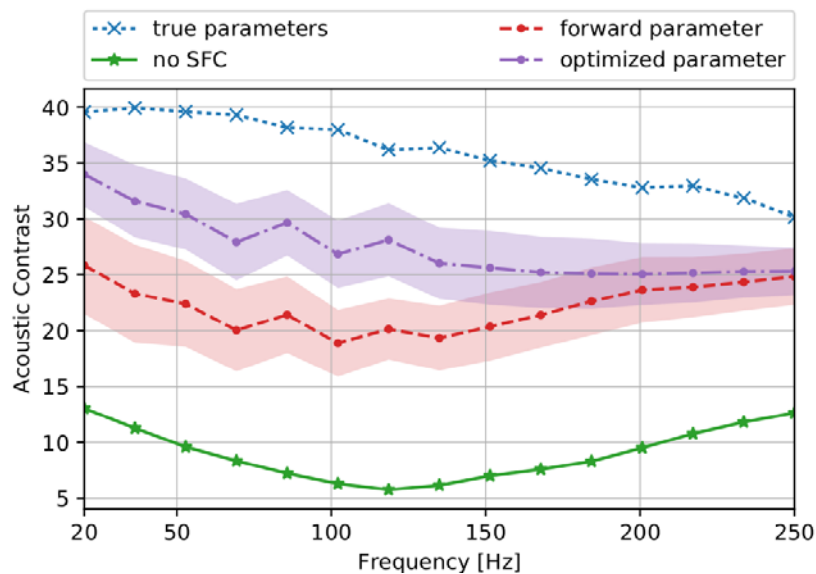


Figure 36: Comparison of acoustic contrast when using true parameters (blue), forward parameters (red), optimized parameter with Bayesian inference (purple) and no SFC (green).

5.5 Measurements

The performance of sound field control solutions is directly dependent on the knowledge of the acoustic transfer functions between the controlled sound system and the areas to be controlled. In outdoor environments, sound propagation is very much affected by the meteorological conditions and its variations. We are investigating the performance of sound field control outdoors, at low frequency, under changing weather conditions. A measurement campaign of one week was carried between the 19th and 28th of November in DTU Campus at Risø, Denmark. Figure 36 shows the setup which mimics a simplified sound field control scenario. The x and y-axes represent East and North respectively. Loudspeakers 1 and 2 (primary and secondary source respectively) were placed 80 m apart. Figure 37 shows one of the loudspeaker units. At a distance of around 300 m, eight microphones were placed in square arrangement with a diagonal size of 50 m.

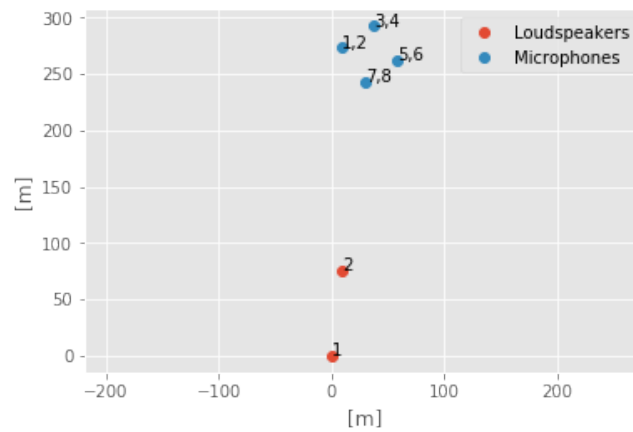


Figure 37: Measurement setup

The sound radiated by the single primary source is mitigated with the secondary source at a single control point at a distance ~ 300 m. The cancellation filter applied to the secondary source is the result of an optimization problem that minimizes the sound pressure produced by both primary and secondary sources at a selected control point (microphone 1). The sound field generated by each loudspeaker and the resulting sound field is also measured at the 7 extra points placed in the vicinity of the control point. The microphones are placed in pairs, one above the ground and one on the ground (Figure 38), to investigate the effect of wind noise on the microphone. Measurements were conducted every 30 minutes for a time period of a week, showing the impact of wind and temperature in the sound propagation and in the resulting sound cancellation. So far we have only analyzed the effect of atmospheric conditions in the propagation of the individual sources, shown in the following subsection.



Figure 38: One of the d&b V-sub units used during the Risø measurements



Figure 39: Microphone arrangement in pairs for each of the recording points

5.5.1 Weather and Sound Propagation

Wind and temperature were gathered during the entire measurement campaign thanks to the collaboration of DTU Wind. A mast with multiple weather sensors placed at [18, 31, 44, 57, 70] m of height logged wind, temperature, and humidity every second. Figure 39 and Figure 40 show logged temperature and wind during the entire measurement period. The temperature range was between -2 and 6°C and the wind direction was primarily coming from the east.

One way of investigating the effect of both wind and temperature on the sound propagation is looking to the change in the propagation delay of the impulse response between each loudspeaker and each microphone. Figure 41 shows the propagation delay as a function of the temperature and the projection of the wind vector on the direction of the sound propagation. It can be noticed that when the wind projection is positive on the direction of the sound and the temperature is higher, the propagation delay is lower, and vice versa.

To prove that this visual correlation is true, a simple linear regression is applied where the time delay is a function of those atmospheric parameters as

$$\tau = a_0 w + a_1 T + a_2 ,$$

where w is the wind projection and T is the temperature. Figure 33 shows an example of interpolation over the entire wind-temperature space [-4, 4] m/s and [-2, 6]°C using the linear regression. We can see that the visual inspection is correct and the delay follows the aforementioned trend with wind and temperature. Figure 42 shows the R^2 error of the linear regression for all the 16 loudspeaker-microphone combinations. A R^2 of 1 means a perfect fit of the data by the model. We can see that the score is very close to one and similar for all the different combinations, implying that this model fits well the data. Finally, the intercept a_2 for the 16 combinations of loudspeaker-microphone is compared in Figure 44 to the distance of the corresponding loudspeaker-microphone pair. It can be seen that there is a linear correlation between them.

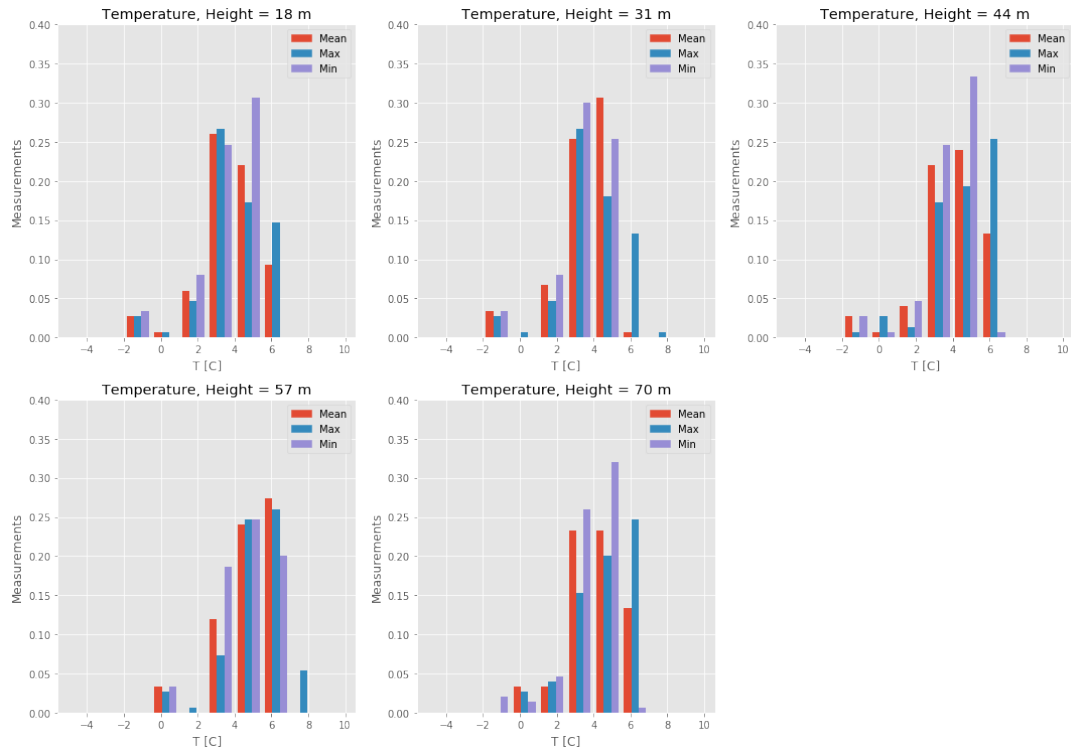


Figure 40: Histogram of the mean, max and min temperature averaged every 10 min for the entire measurement campaign at all heights

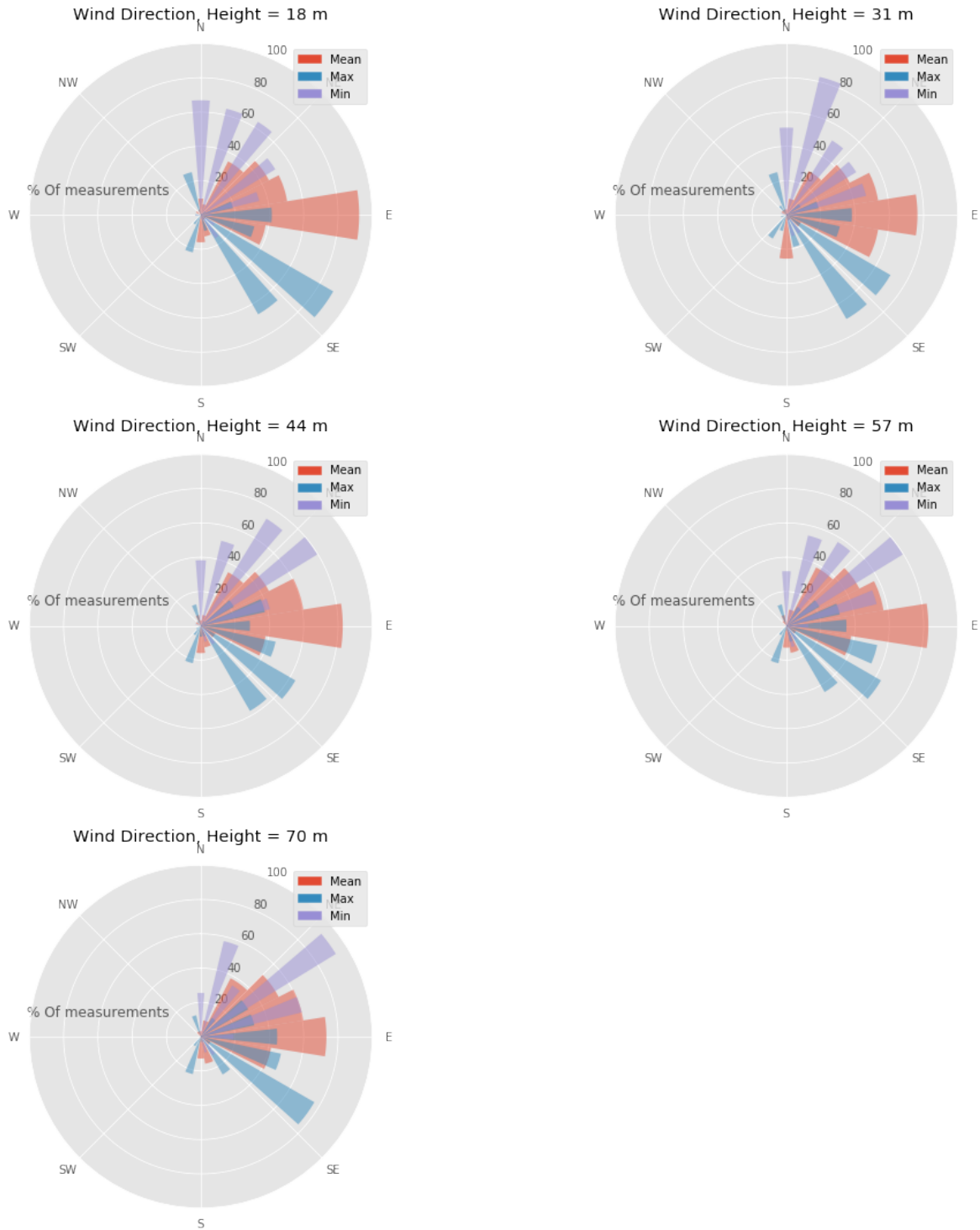


Figure 41: Histogram of the mean, max and min wind direction averaged every 10 min for the entire measurement campaign.

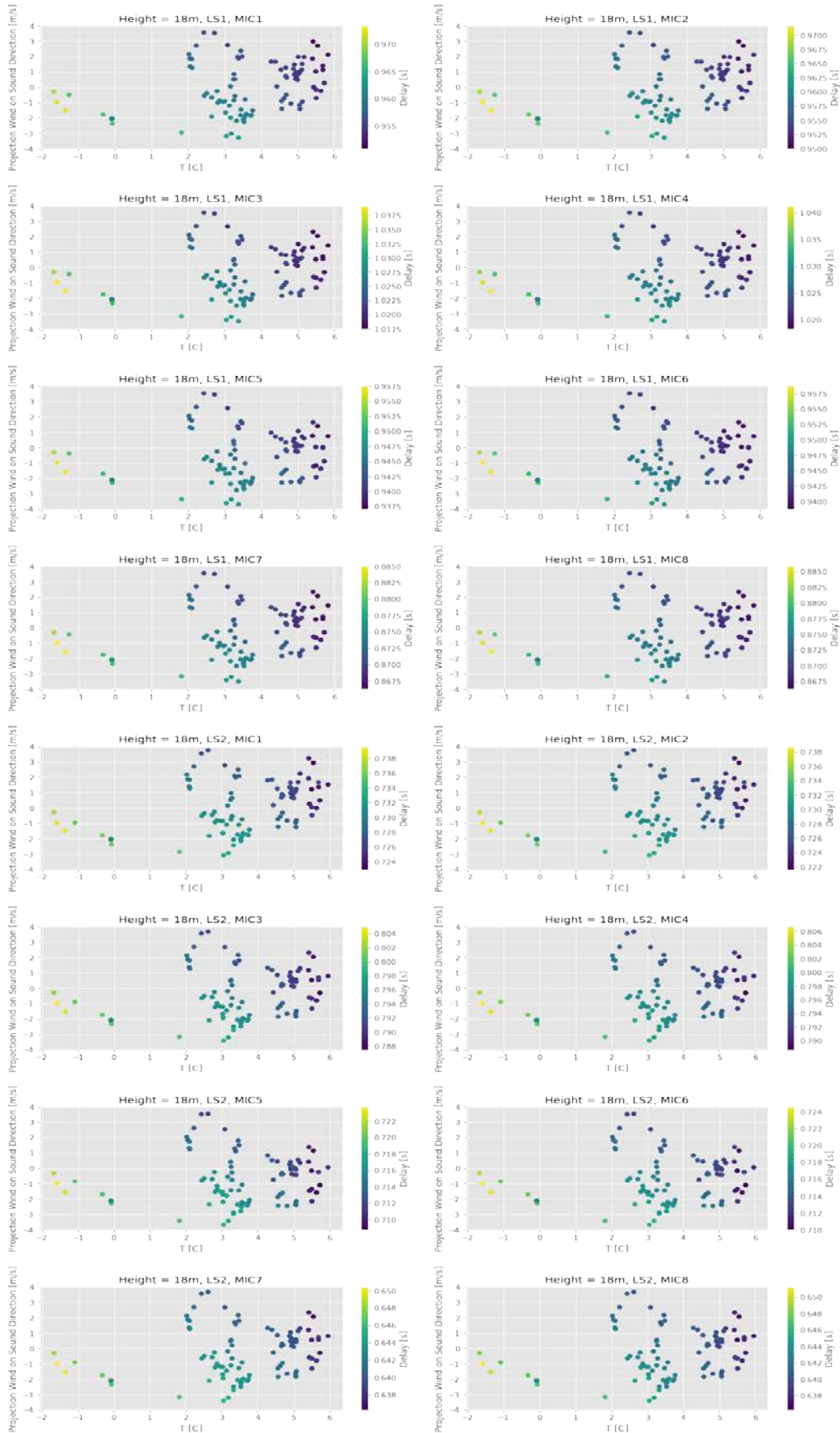


Figure 42: Delay as a function of wind projection and temperature. Results relative to the weather measured at 18m.

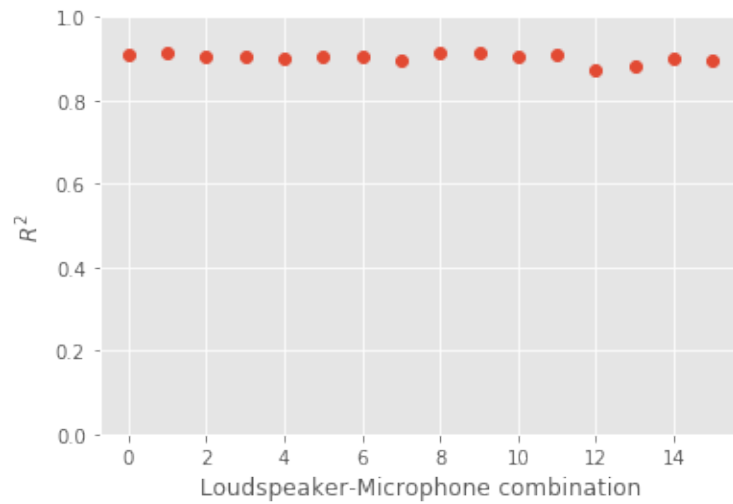


Figure 43: R² error of the regressions for all the combinations loudspeaker-microphone.

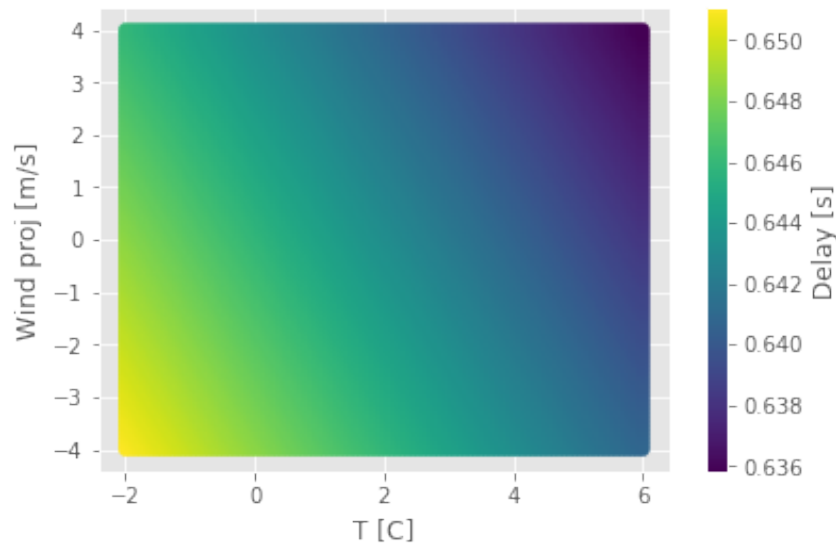


Figure 44: Delay interpolation for loudspeaker 2 and microphone 8

According to these findings we can start working on finding a simplified model that captures all these effects and adapts to them continuously thanks to the IoT network in MONICA.

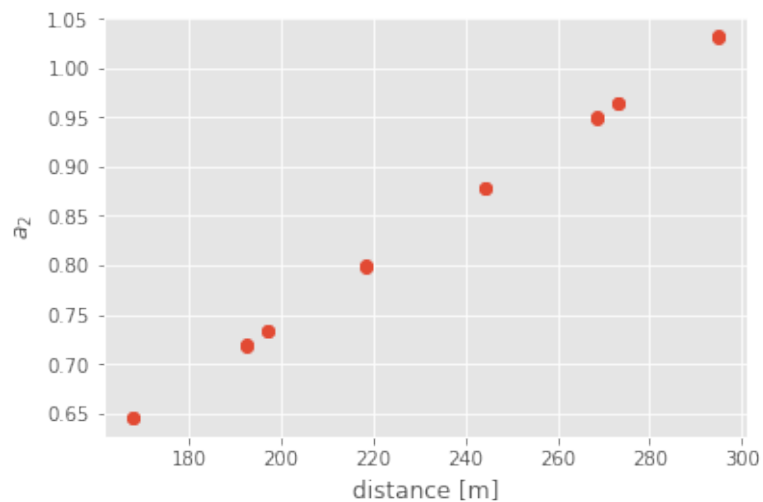


Figure 45: Linear regression intercept vs. distance for each loudspeaker-microphone pair.

5.6 Future work

In regard to the sound zone signal processing, robust optimization techniques based on regularization techniques will be investigated to make the synthesized sound field as robust as possible to changes in the environment and errors in the sound propagation module.

The solutions to the sound zoning problems have so far been computed with frequency domain methods (Chang and Jacobsen, 2012). Solving of these problems in time domain has been shown to be an interesting alternative (Simon Galvez et al., 2015; Møller and Olsen, 2016) and will be investigated for the application in the ASFCS.

5.6.1 Sound Heat Map

One of the problems during the second year has been the implementation of the sound heat map, which is an image calculated via a simplified sound propagation model. DTU already implemented an algorithm that can produce this type of maps as it can be seen in the following picture (Figure 46: Sound Heat Map over Tivoli crowd area.), where Tivoli concert area is simulated including reflecting surfaces such as buildings. However, there has been issues integrating the calculation of the sound heat map in the MONICA cloud which should be finished in the following year.

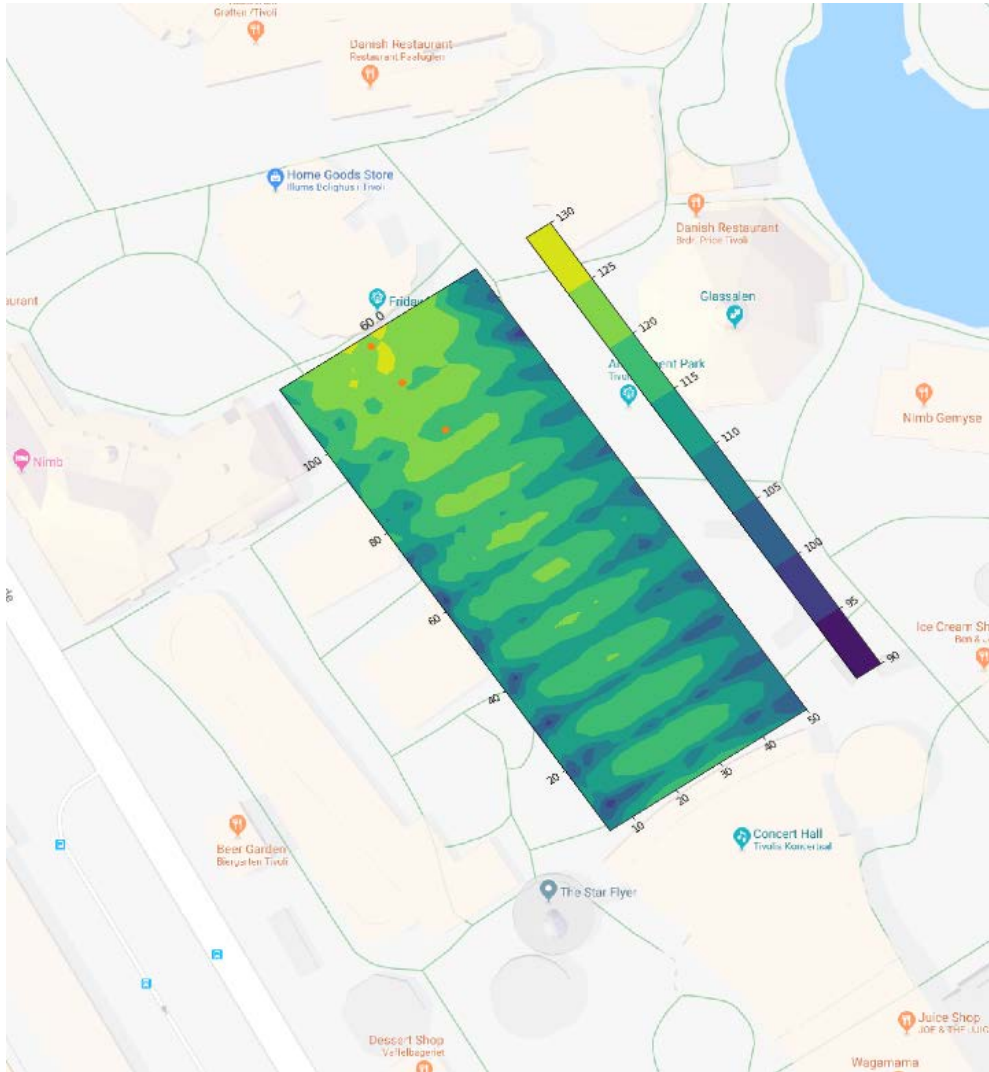


Figure 46: Sound Heat Map over Tivoli crowd area.

6 Noise Monitoring System Configuration (T4.2 and T4.4)

6.1 Technology overview

6.1.1 Noise Monitoring System

The Noise Monitoring System consists of the Source Separation/Contribution techniques (T4.4), the Annoyance measures (T4.4), the Noise Heat Map (Sound Heat Map) (T4.3&4) and the Sound Level Meter (T4.2); the latter, including the first version prototype of the Sound Level Meter as well as its interface with the MONICA Cloud through the Sound Level Meter Gateway, is in detail described in deliverable D4.4 and D4.5, and is thus not further covered here.

Regarding the Source Separation/Contribution techniques, the aim is to estimate the amount of noise contribution (in sound pressure level in dB over time, or similar) that originates from the actual concert in the presence of background noise originating from other noise sources (such as traffic noise, people talking, etc.). Thus, it should answer the question: Is the noise coming from the concert or from other sources?

Two basic approaches are under investigation: the Coherence method and the Pattern recognition approach. In the Coherence method synchronized signal data is obtained from sensors close to the source ('reference' signal), and at locations where people are potentially annoyed, see Figure 46 for an early setup used in the B&K measurement campaign at Tivoli during the summer 2017. The goal is to find the coherent part of the reference signal in the other recordings, and from that to estimate the contribution of the concert. The basic elements and the hardware developed here have been used in the 2018 pilots at Kappa Future Festival and Tivoli, in order to measure synchronized transfer functions over long distances for the ASFC part. In the Pattern recognition approach the goal is to recognize music in the recordings, using machine learning approach, and in this way to estimate the noise contribution. Here no 'reference' signal is needed. On the other hand, the machine learning algorithms will need to categorize sound samples to learn from. This technique will also be used for event detection (gun shot, screams, etc.) in WP6. More details on the Source Separation is given in D4.5.

The Sound Heat Map will give an estimate of the SPL at other positions than the one being measured by the Sound Level Meter. This will be done using the forward sound propagation model developed in T4.3, based on the existing sound propagation model *Nord2000*, see section 5.1.2.



Figure 47: Setup using front-ends for synchronous data, including a GPS antenna for synchronization.

6.1.2 Noise Annoyance Monitoring

The purpose of the Annoyance index is to give a more accurate estimate of noise annoyance, based on subjective perception data.

Acoucity investigated this topic further in 2018. This work allowed better defining the scope of Noise Annoyance Monitoring.

The analysis of acoustic measurements carried on outdoor festivals (Nuits Sonores, Kappa Futur Festival, Festival of Lights and Woodstower) showed that sound emissions at these events have a big amount of energy within the low frequency range (i.e.: from 30 Hz to 250 Hz). In addition to that, results from annoyance survey carried out for the Kappa Futur Festival in July 2017 revealed that:

- Annoyance is associated with noise for more than half of the respondents.
- There is a predominance of low frequencies in the emergence of this discomfort.

Thus, both subjective and physical assessments conclude on the importance of low frequencies in the expressed noise annoyance of outdoor large scale events.

Following these observations, a review of the state-of-the-art was conducted mainly focused on annoyance and low frequency noise. The main findings of this review are:

- Noise annoyance depends on multiple factors, the acoustical dimension being one of them.
- A high inter-individual variability is observed on expressed annoyance of subjects under the same acoustic stimulus.
- Assessment of annoyance based on acoustical measurement can bring to light the main tendencies of community annoyance, but it cannot be used as a predictor of individual annoyance.
- Conventional methods of assessing annoyance, typically based on A-weighted equivalent level, are inadequate for low frequency noise and lead to incorrect decisions by regulatory authorities.
- Weighted level underestimates the effects of low frequency noises.
- Annoyance of low frequencies increases rapidly with level.
- Low frequency noise specific criteria have been introduced in some countries, but do not deal adequately with fluctuations.
- Loudness, and particularly loudness percentile N5 (loudness which is exceeded the 5% of the time of observation) is preferred for describing time varying sounds, take into account of fluctuations.

In order to take into account the aspects previously described, it was decided to investigate loudness of sound recordings of festivals and its correlation with A-weighted and C-weighted sound pressure levels recorded every second. While A-weighted sound pressure levels showed a poor correlation with loudness, C-weighted correlate well with loudness ($R^2 > 0.9$). Even if loudness can provide a most precise description of the acoustical phenomenon in terms of sensorial response, C-weighted values are less time consuming and can be found on most part of sound level meters.

An annoyance index was thus proposed, build on three main rules:

- Easy to understand: linear scale from 0 to 10 (0: no annoyance ; 10: maximum annoyance likelihood)
- Based on C-weighted sound pressure levels
- Comparison between sound levels with and without the event

The proposed annoyance index was tested with measurement during 2018 Nuits Sonores, Kappa Futur and Woodstower festivals with coherent results. However, as noticed in the state-of-the-art, noise annoyance is highly subject to inter-individual variability, so the annoyance index could preferably be renamed as "Annoyance Likelihood Index".

6.2 Services enabled

The Noise Monitoring system is related to the use case Monitor Sound Level.

6.3 Infrastructure and integration with the MONICA IoT platform

We here refer to delivery D4.4 and D4.5, which includes a description of the interface of the Sound Level Meter with the MONICA Cloud through the Sound Level Meter Gateway.

6.4 Measurements

A measurement campaign was performed by B&K and Acoucite during the summer 2017, at and around *Tivoli Fredagrock* in Copenhagen (see Figure 46) as well as in Lyon during *Nuits Sonores*. Two kinds of measurements were performed:

- Synchronized measurements (only at Tivoli): This is done using front-ends (PC & sound card) with GPS synchronization, see Figure 45. One of the devices is the reference (located at the top of the Tivoli Concert Hall). This measurement is done to give input for the Coherence method algorithm development.
- Non-synchronized measurements (Tivoli and Lyon): This is done using Sound Level Meters (SLM) at different places around Tivoli and Lyon to perform audio recordings (wav-files). These are used in the pattern recognition approach, using machine learning algorithms trained by the labeled recorded signals.



Figure 48: Measurements outside Tivoli 2017 using a front-end (left) and a SLM (right)



Figure 49: Non-wired measurements of Transfer Functions at KFF2018 (Left) and Tivoli 2018 (Right). An array of 10 microphones where connected to a B&K frontend equipped with GPS time synchronization.

The technique with GPS synchronized measurements of transfer functions where used in 2018 at the pilots in Kappa Futur Festival and Tivoli, see Figure 47.

6.5 Future work

Measurements at Pilot sites will continue in the coming years. The IoT enabled SLM, described in D4.4 and D4.5, will then be used. Moreover, the developed algorithms will be implemented in the Sound Level Meter Gateway; these algorithms will be tested and adjusted in 2019.

7 Conclusions

We have shown that the ASFCs can considerably increase the acoustic contrast between audience area and the dark zones in the neighbourhood under ideal and real conditions. The sound field control has been successfully applied in outdoor conditions in a controlled scenario in Refshaleøen in Copenhagen presenting results up to 14 dB of sound reduction and in Kappa Futur Festival in Torino with 6 to 8 dB. The performance was not as expected during Friday Rock in Copenhagen, where hardware failures, technical issues and bad weather conditions were present during the entire pilot, which is leading to the model updating techniques that will be used during the 2019 tests.

New alternatives of sound propagation models such as Spherical Harmonics have been investigated, showing promising results in controlled conditions. Further development including atmospheric conditions are under investigation with ongoing measurements campaigns in outdoor conditions. Wind and temperature seem to affect the sound propagation delay in a linear manner, showing the possibility of easily incorporating these conditions in the chosen model.

The development of the Sound Heat Map is lacking the integration in the MONICA cloud, meanwhile the acoustic computations are already implemented. Further collaboration with some of the partners in the project has been scheduled in order to accelerate this process and be ready for the next year.

Furthermore, we have shown that local Quiet Zone system is capable to significantly reduce noise in a local area under laboratory conditions. The experimental validation under real world conditions failed and will be investigated in the future. The computational effort is high for a zone of two square meters and distant reflective surfaces for the noise. In order to increase the quiet zone dimensions, faster algorithms are needed, which is also future work.

8 List of Figures and Tables

8.1 Figures

| | |
|---|----|
| Figure 1: Sketch of the adaptive sound field control system, which is optimized for a good audio experience in the bright zone and low sound pressure level in the dark zone | 10 |
| Figure 2: Information flow in the sound field control system | 12 |
| Figure 3: Infrastructure and deployment of the ASFCs. In full mode the primary loudspeaker system is fed from the Processing Unit. In the Extension Mode the primary loudspeaker system is fed directly from the mixer | 12 |
| Figure 4: Example of ASFCs connected with PA system of the pilot at Tivoli..... | 14 |
| Figure 5: Sketch of the adaptive sound field control system, which is optimized for a good audio experience in the bright zone and low sound pressure level in the dark zone | 15 |
| Figure 6: Comparison of total sound pressure level in the vicinity of the simulated venue, small dark zone. | 16 |
| Figure 7: Comparison of total sound pressure level in the vicinity of the simulated venue for the small dark zone case | 17 |
| Figure 8: Comparison of total sound pressure level in the vicinity of the simulated venue, surrounding dark zone | 18 |
| Figure 9: Comparison of total sound pressure level in the vicinity of the simulated venue for the surrounding dark zone case | 18 |
| Figure 10: Measurement setup for loudspeaker characterization | 19 |
| Figure 11: Modelled and measured response of the loudspeaker under test at the microphone positions together with the relative error. Note that the phase is back-propagated in time and unwrapped for a clearer presentation and readability. | 20 |
| Figure 12: Photo of small scale anechoic experiment setup | 21 |
| Figure 13: (Top) Insertion loss of sound field control system in anechoic experiment. Higher values indicate a larger reduction of sound pressure level in the dark zone. (Bottom) primary to secondary ratio in anechoic experiment. Higher values indicate less distortion by control loudspeakers in bright zone. | 22 |
| Figure 14: No control: magnitude of sound sound field in bright (left) and dark zone (right) at three frequencies. Primary sources are at $x=0$. The secondary sources in between the two zones. | 23 |
| Figure 15: With control: magnitude of sound field in bright (left) and dark zone (right) at three frequencies. Primary sources are at $x=0$. The secondary sources in between the two zones. | 24 |
| Figure 16: Photo of large scale outdoor experiment setup..... | 25 |
| Figure 17: Performance metrics at outdoor experiment. (Top) insertion loss. (Bottom) primary to secondary ratio. | 26 |
| Figure 18: Control subwoofer at Kappa Futur Festival 2018. The festival stage can be seen in the back. | 27 |
| Figure 19: Arrangement of control sources and microphones at Kappa Futur Festival 2018..... | 28 |
| Figure 20: Performance at Kappa Futur Festival 2018. | 29 |
| Figure 21: Control array at Tivoli 2018 pilot. The courtyard of the building in the background was used as the dark zone. | 30 |
| Figure 22: A possible use case of quiet zone systems in a loud outdoor venue..... | 31 |
| Figure 23: Prototype of the Quiet Zone System tested at the Tivoli pilot site. The controller and the error microphones are not shown here. Error! Bookmark not defined. | |
| Figure 24: Multichannel Controller Architecture. X : Reference signal (from mixing engineers console), W_{ii} FIR filters, M_i Secondary loudspeakers, S_{ii} sound propagation paths, E_i : Error measurement positions. | 32 |
| Figure 25 Technical Architecture of the Quiet Zone system (active part). | 33 |
| Figure 26: Information flow chart, ASFC including the Quiet Zone. | 34 |
| Figure 27: Results from Simulations. This plot shows the Insertion loss in the quiet zone (colored area). Red circles on the left: the venue loudspeakers, red circles in the middle: control speakers, black crosses: error microphones. The insertion loss averaged over the whole zone is 14.25 dB. | 35 |
| Figure 28: Measured Insertion Loss in Quiet Zone, red dots: measurement positions, black circles: control sources, black crosses: error microphones | 35 |
| Figure 29: Vertically measured Insertion Loss, up to 10 dB attenuation 30cm above the microphone array. | 36 |
| Figure 30: Extracted transfer functions from an Error Mic and a Reference Mic. | 37 |
| Figure 31: Signal processing flow of the Sound Field Controller, which is a module shown in Figure 2. | 39 |
| Figure 32: IL comparison between using 1400 microphones and 16 microphones with the spherical harmonics model. | 40 |
| Figure 33: Setup with 1400 microphones (white) and 18 loudspeakers (red). In blue the 16 microphones to fit the model and reconstruct the transfer functions. | 40 |

| | |
|---|----|
| Figure 34: Setup of bright zone, dark zone and fixed loudspeaker positions in the simulation. | 41 |
| Figure 35: Comparison of acoustic contrast when using true parameters (blue), forward parameters (red), optimized parameter with Bayesian inference (purple) and no SFC (green). | 42 |
| Figure 36: Measurement setup..... | 43 |
| Figure 37: One of the d&b V-sub units used during the measurements | 43 |
| Figure 38: Microphone arrangement in pairs for each of the recording points..... | 44 |
| Figure 39: Histogram of the mean, max and min temperature averaged every 10 min for the entire measurement campaign at all heights..... | 45 |
| Figure 40: Histogram of the mean, max and min wind direction averaged every 10 min for the entire measurement campaign. | 46 |
| Figure 41: Delay as a function of wind projection and temperature. Results relative to the weather measured at 18m. | 47 |
| Figure 42: R ² error of the regressions for all the combinations loudspeaker-microphone. | 48 |
| Figure 43: Delay interpolation for loudspeaker 2 and microphone 8..... | 48 |
| Figure 44: Linear regression intercept vs. distance for each loudspeaker-microphone pair..... | 49 |
| Figure 45: Setup using front-ends for synchronous data, including a GPS antenna for synchronization. | 51 |
| Figure 46: Measurements outside Tivoli using a front-end (left) and a SLM (right) | 53 |
| Figure 47: Non-wired measurements of Transfer Functions at KFF2018 (Left) and Tivoli (Right) | 53 |

8.2 Tables

| | |
|--|----|
| Table 1: Comparison of operation modes | 11 |
| Table 2: Nord2000 model parameters..... | 42 |

9 References

- Betlehem, Terence, Wen Zhang, Mark A. Poletti, and Thushara D. Abhayapala. 2015. "Personal Sound Zones: Delivering Interface-Free Audio to Multiple Listeners." *IEEE Signal Processing Magazine* 32 (2):81–91. <https://doi.org/10.1109/MSP.2014.2360707>.
- Chang, Ji-Ho, and Finn Jacobsen. 2012. "Sound Field Control with a Circular Double-Layer Array of Loudspeakers." *The Journal of the Acoustical Society of America* 131 (6):4518–25. <https://doi.org/10.1121/1.4714349>.
- Chang, Ji-Ho, and Finn Jacobsen. 2013. "Experimental Validation of Sound Field Control with a Circular Double-Layer Array of Loudspeakers." *The Journal of the Acoustical Society of America* 133 (4):2046–2046. <https://doi.org/10.1121/1.4792486>.
- Choi, Joung-Woo, and Yang-Hann Kim. 2002. "Generation of an Acoustically Bright Zone with an Illuminated Region Using Multiple Sources." *The Journal of the Acoustical Society of America* 111 (4):1695–1700. <https://doi.org/10.1121/1.1456926>.
- Farina, Angelo. 2007. "Advancements in Impulse Response Measurements by Sine Sweeps." *Proc. 122nd AES Convention*, 1–21.
- Feistel, Stefan. 2014. *Modeling the Radiation of Modern Sound Reinforcement Systems in High Resolution*. Berlin: Logos-Verl. <http://publications.rwth-aachen.de/record/444852>.
- Heuchel, Franz M, Caviedes Nozal, Diego, Jonas Brunskog, Efren Fernandez Grande, and Finn T Agerkvist. 2017. "An Adaptive, Data Driven Sound Field Control Strategy for Outdoor Concerts." In *Audio Engineering Society Conference: 2017 AES International Conference on Sound Reinforcement – Open Air Venues*. <http://www.aes.org/e-lib/browse.cfm?elib=19181>.
- Heuchel, F., Caviedes Nozal, D., and Agerkvist, F.T. 2018. "Sound field control for reduction of noise from outdoor concerts." in *Proc. 145th Audio Engineering Society Convention*, NY, USA. http://orbit.dtu.dk/files/160467692/AES_2018_Sound_field_control_for_reduction_of_noise_from_outdoor_concerts_1_.pdf
- Hansen, Colin, Snyder Scrott et. al. 2012 "*Active Control of Noise and Vibration*", CRC Press
- Jacobsen, Finn, and Peter Møller Juhl. 2013. *Fundamentals of General Linear Acoustics*. Wiley. <https://doi.org/10.1017/CBO9781107415324.004>.
- Kuo, Sen S. and Morgan, Dennis R. 1996. "*Active noise control systems: algorithms and DSP implementations*", Wiley
- Moreau, Danielle et al. 2008. "*A review of virtual sensing algorithms for active noise control*", *Algorithms*, 1, 69-99
- Møller, Martin Bo, and Martin Olsen. 2016. "Sound Zones: On Performance Prediction of Contrast Control Methods." In *Audio Engineering Society Conference: 2016 AES International Conference on Sound Field Control*, 0–13. <http://www.aes.org/e-lib/browse.cfm?elib=18308>
- Ophem, S. van and Berkhof, A. P. 2013. "*Multi-channel Kalman filters for active noise control*", *The Journal of the Acoustical Society of America* 133, 2105. <https://doi.org/10.1121/1.4792646>
- Plovsing, Birger. 2006 "Nord2000. Validation of the Propagation Model". *AV 1117/06, A550054, DELTA*.

Simon Galvez, Marcos F., Stephen J. Elliott, and Jordan Cheer. 2015. "Time Domain Optimization of Filters Used in a Loudspeaker Array for Personal Audio." *IEEE/ACM Transactions on Audio, Speech, and Language Processing* 23 (11):1869–78.

<https://doi.org/10.1109/TASLP.2015.2456428>.

Tabatabaei Ardekani, Iman and Abdulla, Waleed H. 2011. "*FxLMS-based Active Noise Control: A Quick Review*", APSIPA ASC http://www.apsipa.org/proceedings_2011/pdf/APSIPA260.pdf

Caviedes Nozal, Diego, and Brunskog, Jonas. 2018. "*Parameter optimization of forward sound propagation models using Bayesian inference for sound field control purposes*" 2018 *Euronoise 2018 Proceedings* . p. 2301-2308